Spring 4-24-2015

Mechanical and Physical Property Characterization of Macroporous Recycled-Aggregate Pervious Concrete

Patrick William Barnhouse
University of Colorado at Boulder, pbarn1338@outlook.com

MECHANICAL AND PHYSICAL PROPERTY CHARACTERIZATION OF MACROPOROUS RECYCLED-AGGREGATE PERVIOUS CONCRETE

By
PATRICK WILLIAM BARNHOUSE
B.S., Marquette University, 2013

A thesis submitted to the
faculty of the Graduate School of the
University of Colorado in partial fulfillment
of the requirements for the degree of
Master of Science
Department of Civil, Environmental, and Architectural Engineering

2015

This thesis entitled:
Mechanical and Physical Property Characterization of Macroporous Recycled-Aggregate Pervious Concrete
Written by Patrick William Barnhouse
has been approved for the Department of Civil, Environmental and Architectural Engineering

____
Wil V. Srubar III

____
Mija H. Hubler

____
Yunping Xi

Date__________________

The final copy of this thesis has been examined by the signatories, and we
find that both the content and the form meet acceptable presentation standards
of scholarly work in the above mentioned discipline.

Barnhouse, Patrick William (M.S., Civil, Environmental, and Architectural Engineering)

Mechanical and Physical Property Characterization of Macroporous Recycled-Aggregate Pervious Concrete

Thesis directed by Professor Wil V. Srubar III

Pervious concrete has been widely used in pavement applications to help alleviate environmental issues related to urban stormwater runoff and pollution. While horizontal infrastructure (e.g., pavements) represent the majority of applications over the past few decades, pervious concrete is now being considered for other building infrastructure applications, such as sound barriers, insulation, and vertical garden walls. These new applications necessitate different physical and mechanical properties (e.g., ultra-high porosities) than pervious pavements. In response to this need, this research defines macroporous pervious concrete (MPC) as a pervious concrete with a minimum porosity of 30% and proposes it as a possible material solution for these new applications. The objective of this work was to characterize the mechanical and physical properties of the MPC under simulated field conditions. Due to the anticipated low strength of ultra-high porosity concrete, the impact of two binder additives, namely sand and titanium dioxide (TiO_2), on the compressive strength of MPC was investigated. In addition, the effect of recycled aggregates on the mechanical and physical properties was assessed herein. To compare permeability of MPC to normal (< 30% porosity) pervious concrete, a modified Carman-Kozeny equation was proposed to predict permeability. Results demonstrate that MPC has a lower compressive strength and higher permeability than normal pervious concrete. Additionally, the use of recycled aggregates in lieu of virgin aggregates in MPC does not compromise its mechanical properties, but does impact MPC physical properties. Rather than being controlled by the parameters of unit weight, porosity, and aggregate type that usually govern the mechanical properties of normal pervious concrete, the strength of the MPC binder solely governs its mechanical performance. Furthermore, the data show that cement-binder additions of 7% sand or 2.5% TiO_2 improve compressive strengths of recycled-aggregate MPC by 19% and 7%, respectively and that simultaneous use of both additives increase MPC compressive strength by 28%.

DEDICATION

This thesis is dedicated to everyone who has ever believed in me. Your love, guidance, support and unwavering hope has sustained me through trials and difficulties. Each of you has been my rock and I could not have done it without you.

Especially you, Mom and Dad.

ACKNOWLEDGEMENTS

I would first like to thank my advisor, Dr. Wil V. Srubar for his outstanding guidance and mentorship. His optimism and passion for materials and sustainability is infectious. Additionally, I want to thank Dr. Srubar and the Sustainable Infrastructure Materials Laboratory (SIMLab) within the Department of Civil, Environmental and Architectural Engineering and the College of Engineering and Applied Sciences at the University of Colorado Boulder for providing the funding necessary to make this research possible.

I also want to take the opportunity to give thanks for the assistance of Mr. Luke Traeger and Mr. Ethan Gormican at the University of Colorado Boulder in preparing and handling the recycled aggregates. I am also thankful for the opportunity to meet Mr. Bill Kepler, Mr. Bruce Shulte, and Mr. Fred Travers at the United States Bureau of Reclamation and for their willingness to allow me to carry out testing of the concrete cylinders. Lastly, I am grateful to Mr. Randy Ehmer of DuPont and Mr. Tom Pelo of BASF for their donation of materials.

Contents

Chapter 1 Introduction

Over the past several decades, there has been a growing interest in green infrastructure and sustainable materials. As a result, there has been a growing interest in pervious concrete because of its well-known environmental benefits in improving the quality and reducing the quantity of urban stormwater runoff. Pervious concrete contains cement, coarse aggregate, and water but little to no fine aggregate (ACI 522R-10). This lack of sand or any other fine aggregate allows for the development of a network of interconnected pores which permits the flow of water through the concrete. This network of pores typically generates a porosity that ranges from 15 to 30% (ACI 522R-10). The porosity, or air void content, of pervious concrete directly controls multiple other properties of the material. Relationships have been studied and well defined between porosity and unit weight, porosity and compressive strength, and porosity and permeability. In general, it is known that as porosity increases, unit weight and compressive strength decrease while permeability increases (Meininger 1988; Mulligan 2005). Because of its porous nature, the compressive strength of pervious concrete is also less than normal concrete. Generally, pervious concrete compressive strengths vary from 1000 to 3000 psi (6.9 to 20.7 MPa) for the typical porosity range with lower strengths coming from higher porosity concretes.

Pervious concrete materials have a high potential to be a sustainable component of green infrastructure. There are several current areas of research to improve the sustainability and resilience of pervious concrete. These efforts include: (1) enhanced freeze-thaw durability, as this is a critical form of deterioration, particularly in regions where complete saturation may occur before freezing (ACI 522R-10); (2) internal curing, which works to enhance cement hydration to provide improved mechanical and durability properties (Kevern and Farney 2012); and (3) geopolymers, an alternative to portland cement that contains less embodied energy and performs comparably to typical cement-based pervious concretes (Tho-in and Sata 2011). The development of standards for pervious concrete is also a topic of interest. Currently, only four (4) ASTM standards exist for pervious concrete, including ASTM C1688, for the measurement of voids in fresh pervious concrete, ASTM C1701 as a method to test the infiltration rate of in-place pervious concrete, ASTM C1747 as a means to determine the potential abrasion resistance of pervious concrete, and ASTM C1754 for the measurement of voids in hardened pervious concrete.

The research herein is focused on yet another research area, namely, alternative applications of pervious concrete. Pervious concrete has been primarily applied in permeable pavement applications. However, the acoustic, thermal and physical properties of the material have sparked interest in pervious concrete for non-pavement applications such as drain tiles and solar heating systems (Ghafoori and Dutta 1995). Even though research has begun in the area of alternative applications, no intentional research has yet been done on a material for such applications. This research seeks to characterize the properties of a type of pervious concrete suitable for non-pavement applications.

This thesis will follow an outline of two (2) papers that are being submitted for publication in peer-reviewed journals. Chapter 2 is a review of the current body of knowledge for several design considerations and constituent materials for pervious concrete along with an explanation for the growing popularity of the material. This will be followed by Chapter 3, which details the materials and methods used to carry out the research conducted on a pervious concrete for non-pavement applications. The results and conclusions obtained are discussed in Chapter 4, and Chapter 5 concludes with a discussion of possible topics for future research.

Chapter 2 Literature Review

2.1 Pervious Concrete Benefits

Pervious concrete has gained much interest in recent years due to its many hydrological and urban health benefits. As a porous and permeable pavement, as the material is typically utilized, pervious concrete is capable of reducing stormwater volumes via direct infiltration (Welker, Barbis, and Jeffers 2012). This reduction in stormwater volumes can then reduce the size or eliminate the need for storm sewers (ACI 522R-10). Pervious concrete not only affects the quantity of stormwater, but it also improves the quality. It does so by lowering the concentrations of heavy metals such as copper, lead, chromium, cadmium and zinc (Welker, Barbis, and Jeffers 2012). In addition to its impact on stormwater, pervious concrete also reduces the urban heat island effect. In spite of the fact that it has a higher surface temperature than normal concrete, the insulating properties of pervious concrete reduce heat transfer by 41% and allow the material to be cooler overall (Haselbach 2009). The heat is further mitigated through the evaporative cooling effect of collected rainwater evaporating (Haselbach et al. 2011). Along with reducing the urban heat island effect, the insulating properties of pervious concrete also help to reduce the thermal pollution that enters local rivers, streams and lakes (Haselbach et al. 2011). Overall, these benefits lead to reduced urban health problems related to heat strokes in urban areas and to decreased degradation of aquatic ecosystems (Haselbach et al. 2011; Starke, Gobel, and Coldeway 2010; Nemirovsky, Welker, and Lee 2013; Goel 2006). To achieve a pervious concrete with the described benefits, a few design parameters must be considered. They are freeze-thaw durability, compaction and permeability.

2.2 Design Considerations

The first parameter typically considered in the design of pervious concrete materials is permeability. As previously mentioned, permeability is directly related to porosity, that is, as porosity increases, permeability does as well. A common method of modeling and predicting this relationship is the Carman-Kozeny equation (Kevern and Schaefer 2013; Montes and Haselbach 2006; Neithalath 2004). The equation frequently used in the literature is given in Equation 1.

$$K = \alpha\left[\frac{p^3}{(1-p)^2}\right] \quad \text{(Eqn. 1)}$$

Where K is the permeability of the pervious concrete in cm/s, p is the porosity in terms of percentage and α is an empirical coefficient used to simplify the relationship. Equation 1 is in the form of a Carman-Kozeny equation developed by Bayles, et al. (Bayles, Klinzing, and Chiang 1989). In their study, Xu and Yu (2008) list ten (10) modifications to this equation, of which the Bayles, et al. form is one. Within this form commonly used for pervious concrete, there is also variation of the α value. For example, Kevern and Schaefer (2013) use a value of 30, while Montes and Haselbach (2006) use a value of 18. The variability of the coefficient highlights the inconsistencies that exist in this empirical modeling approach. Alternatively, in place of α, a pore shape factor (F_s), pore specific surface area (S_0) and tortuosity (τ) can be used as in Equation 2 (Neithalath 2004). This eliminates the empirical value but increases the complexity of the equation. One of the added variables, tortuosity, is the degree of connectivity of the pervious concrete pore system and is known to have an important factor on permeability (ACI 522R-10).

$$K = \left(\frac{1}{F_s \tau^2 S_0^2}\right)\left[\frac{p^3}{(1-p)^2}\right] \quad \text{(Eqn. 2)}$$

Other factors impact permeability as well. One factor is the aggregate size of the pervious concrete. As aggregate size increases, permeability also increases (Mitchell et al. 2011). Another factor is the condition of the soil on which the pervious concrete is cast. Base soils should generally have a percolation rate of at least 0.5 in/hr (13 mm/hr) to a depth of 4.0 ft (1.2 m) any interference with the percolation of the water through the concrete (ACI 522R-10).

A second design consideration is the type and amount of compaction applied during the casting of pervious concrete. Compaction energy is critical to pervious concrete because it controls the porosity, which in turn controls multiple other properties as described in Chapter 1. A lower compaction energy causes reduced unit weight, compressive strength, tensile strength and increased porosity and permeability (Suleiman et al. 2006). In the field, compaction typically occurs via a roller or vibrating screed (ACI 522.1-13); however, this is not practical for most lab-based testing. Because of this, conventional cylinder molds are commonly used. In their study, Putnam and Neptune (2011) investigated eight (8) types of cylinder compaction methods that were grouped into rodding, Proctor hammer compaction, and dropping the mold. They found that Proctor hammer compaction was able to give porosity and density results closest to field core samples, but the cylinder density was still greater than the field core density

(Putman and Neptune 2011). In another study on compaction methods for pervious concrete, it was found that a pneumatic press that applied approximately 10 psi (0.07 MPa) to an overfilled mold was able to achieve very similar results to field core samples (Mahboub et al. 2009). In ASTM C1688, two methods of pervious concrete consolidation are prescribed. For both methods, the concrete is added in two, approximately equal, lifts. The first method consolidates each lift of the pervious concrete with twenty (20) drops of a Standard Proctor hammer. The second method is similar with compaction being completed with ten (10) drops of a Marshall hammer per lift.

Another design consideration is freeze-thaw durability. Multiple authors have investigated this topic as it relates to pervious concrete. Vancura, et al. (2011) completed a survey of thirty-three (33) pervious concrete samples and found that the cracking patterns of freeze-thaw damage in pervious concrete appeared similar to confirmed freeze-thaw damage in standard concrete. Vancura, et al. found cracking to go through the aggregate, paste and interfacial transition zone (ITZ). Additionally, despite the use of an air entraining agent for all concretes surveyed, no sample had sufficient entrained air for freeze-thaw durability (Vancura, MacDonald, and Khazanovich 2011). The authors noted that this may not be a large concern for pervious concrete because the w/c ratio for the material is generally low, which also improves long-term durability.

A study of freeze-thaw durability by Kevern and Sparks (2013) examined the impact of internal curing via superabsorbent polymers and of cost effective remediation strategies, namely latex paint, epoxy, and a surface densifier. It was found that pervious concretes with internal curing agents performed better than those without. Additionally, Kevern and Sparks noted that the epoxy provided the best protection from freeze-thaw deterioration, that is surface raveling followed by the paint and surface densifier, respectively. The most cost effective method to prevent freeze-thaw damage was found to be the use of a superabsorbent polymer for internal curing.

A novel method of freeze-thaw testing was completed by Yang where the author deviated from the typical cycling prescribed in the ASTM 666 standard for freeze-thaw testing and completed only one freeze-thaw cycle per day (Yang 2011). Additionally, specimens were either water cured or air cured in ambient conditions to represent field conditions. This simulation of field conditions proved important for two reasons. First, Yang found that the air curing method reduced the freeze-thaw durability of the samples. Additionally, an addition of silica fume to the mix design improved the performance of the water cured specimens while it detracted from the durability of the air cured samples (Yang 2011). It was also shown that the addition of polypropylene fibers enhanced the resistance of the concrete to freeze-thaw deterioration.

2.3 Pervious Concrete Materials

The constituent materials that make up pervious concrete, that is, coarse aggregate, cement, water, and a limited amount of fine aggregate, contribute to the macroscopic properties of the pervious concrete. Water reducing admixtures are beneficial and commonly used as they help maintain sufficient workability for the pervious concrete which typically has a low water-to-cement ratio (0.26 to 0.40) (ACI 522R-10).

The aggregate used in pervious concrete impacts performance. In a study of seventeen (17) types of aggregate, granite and river gravel were found to yield a more durable pervious concrete (Kevern, Wang, and Schaefer 2010). Kevern, et al. (2010) also noted that aggregates with a high absorption or low specific gravity tended to yield a pervious concrete with less freeze-thaw durability. The authors also indicated that a small addition of sand improved freeze-thaw durability. Lastly, it was found that angular aggregates tended to give a porosity higher than that which was designed while rounded aggregate typically gave the designed porosity (Kevern, Wang, and Schaefer 2010). An increase in bulk volume of aggregate also led to an increase in porosity and a decrease in compressive strength and modulus of elasticity (Crouch, Pitt, and Hewitt 2007). The loss in mechanical properties was attributed to a decrease in paste content at higher aggregate volumes and indicated the importance of paste to pervious concrete (Crouch, Pitt, and Hewitt 2007). Crouch, et al. also found a similar trend for mechanical properties when pervious concrete aggregates were replaced with larger aggregates.

In addition to their benefits to freeze-thaw durability, superabsorbent polymers and sand improved the overall performance of pervious concrete (Kevern and Schaefer 2013). A study found that a pervious concrete mix with No. 4 (4.75 mm) aggregate, a 7% replacement of coarse aggregate with sand and air entrainer to lose less than 2% of its mass after freeze-thaw testing and to be the best performing (Kevern et al. 2008). In this study, the addition of sand only marginally reduced the permeability of the concrete.

Recycled concrete aggregate (RCA) has also been studied in pervious concrete. At a 100% replacement of virgin aggregate with RCA, Berry, et al. (2012), Gaedicke, et al. (2014), and Rizvi, et al. (2010) have recorded compressive strength losses of 16%, 15% and 43%, respectively. RCA has also been found to be more sensitive to the difference of laboratory cylinder molds and field slabs (Gaedicke, Marines, and Miankodila 2014). RCA has also been noted to be absorptive and can increase the capillary water absorption of pervious concrete by 50% (Tittarelli, Carsana, and Ruello 2014). Additionally, the acoustic properties of pervious concrete were found not to be diminished by the use of RCA (Park, Seo, and Lee 2005).

2.4 TiO_2 Applications in Cement-Based and Concrete Materials

One of the many additives that have been studied in pervious concrete is titanium dioxide (TiO_2). TiO_2 has been widely lauded as a photocatalytic additive for cement-based materials. As a photocatalyst, TiO_2, in the presence of UV radiation, is able to induce a redox reaction on adsorbed substances which can effectively remove pollutants from the air and water, and it also induces high levels of hydrophilicity (Chen and Poon 2009). Particularly, the degradation of NO_x across concrete products with TiO_2 has been studied by multiple authors (Ballari et al. 2010; Hüsken, Hunger, and Brouwers 2009). Volatile organic compound (VOC) removal has also been proven possible. In a comparison of the surface application via dip-coating or sol-gel methods, dip-coating was seen to be more effective at removing VOCs from the environment (Ramirez et al. 2010). It has also been recorded that TiO_2 is still photocatalytic and able to provide benefits when it is part of the cement paste or mortar mix and not only applied to the surface of the material (Ruot et al. 2009).

These photocatalytic benefits have also been studied not just for concrete and cement-based materials in general but for pervious concrete specifically. In a study of the surface treatment of pervious concrete with TiO_2, it was observed that the material was more efficient at NO_x removal than it was at VOC removal. Additionally, pervious concrete with TiO_2 had a NO_x removal efficiency that ranged from 34 to 62% and was seen to decrease with higher humidity levels and pollutant flow rates (Asadi et al. 2012).

The observed benefits of TiO_2 have not been limited to those associated with its photocatalytic activity. In addition, there have been multiple authors that have noted mechanical benefits due to enhanced cement hydration. TiO_2 has been found to specifically enhance the degree of hydration for belite (C_2S) by approximately 47% at 90 days (Lee and Kurtis 2012). Lee and Kurtis also noted that an enhanced hydration of belite could reduce the energy consumption of cement production by reducing the need fire clinker to the point of alite (C_3S) formation. In a study investigating TiO_2 on overall portland cement hydration, the use of TiO_2 was again seen to enhance hydration (Jayapalan, Jue, and Kurtis 2014). Jayapalan, et al. proposed that TiO_2 enhanced the rate and degree of hydration via the heterogeneous nucleation effect where the TiO_2 particles provided additional nucleation sites for hydration to occur. In the same way, silica fume and nano-silica are known to act as nucleation sites for the precipitation of calcium silicate hydrate (CSH) in the cement paste due to the small particle size of the material (Qing et al. 2007). These hydration findings were applied by Chen, et al. (2012) where two types of TiO_2, anatase and an anatase-rutile blend, were found to decrease the setting time and increase the compressive strength of mortar cube specimens. The TiO_2 was dosed at 5 and 10% additions by weight of cement with the 10% addition showing diminished returns.

2.5 Non-Pavement Applications

The existing literature described in Sections 2.1 through 2.4 is representative of the extensive research that has been conducted on pervious concrete. However, most applications for pervious concrete have focused on horizontal infrastructure, namely permeable pavements. However, there is increasing interest in using pervious concrete in other applications as well. Historically, pervious concrete was used as an economic building material in post-World War II Europe since it contained less cement per unit volume than normal concrete (Ghafoori and Dutta 1995). Modern applications in transportation and building infrastructure have begun to utilize the acoustic and thermal properties of pervious concrete in sound barriers and reinforced insulation panels (Carsana, Tittarelli, and Bertolini 2013). Ghafoori and Dutta (1995) have recently identified novel uses of pervious concrete in drainage systems, tennis courts, and components of solar heating systems. In Japan, the porous nature of pervious concrete was exploited in the design of “biohabitats” for supporting a diverse array of plants, insects, marine organisms, and microbes (Tarnai et al. 2003). Non-structural applications of pervious concrete require different properties to suit a wide range of material requirements. For example, the requirements for durable permeable pavements (e.g., high strength, ~20% porosity) may not be appropriate in other applications, like insulation panels or biohabitats, where higher porosities are favored over mechanical properties. While the majority of pervious concrete materials research completed to-date has been primarily limited to pavement materials with porosities that range from 15-30%, there have been a few isolated studies that reported outlier samples with porosities greater than 30% (Kevern 2014; Jang et al. 2015).

2.6 Scope of Work

The objective of this study was to characterize the mechanical, physical, and hydraulic properties of macroporous pervious concrete (MPC), which is defined herein as pervious concrete with a minimum porosity (air void content) of 30%. The effect of incorporating recycled concrete aggregates (RCA) on the properties of MPC was also investigated herein. According to the Federal Highway Administration, RCA is primarily used for aggregate road base and only eleven states permit the use of RCA as an aggregate for new concrete projects (FHWA, 2004). As explained in Section 2.3, a few studies have explored the use of RCA in pervious concrete, but the body of literature is not extensive. Nonetheless, multiple authors have reported that the incorporation of RCA reduces compressive strength of pervious concrete (Berry et al. 2012; Gaedicke, Marines, and Miankodila 2014; Rizvi et al. 2010). For example, at a 100% replacement of RCA, Berry, et al. (2012), Gaedicke, et al. (2014), and Rizvi, et al. (2010) have recorded compressive strength losses of 16%, 15% and 43%, respectively.

Due to ultra-high porosities and the incorporation of RCA, low compressive strengths and higher sensitivities to field-condition curing (rapid evaporation) was anticipated (ACI 522R-10). Thus, methods to maintain or improve the mechanical performance of MPC were explored. The need for an improved paste strength and paste-aggregate interface in pervious concretes has been previously identified (Kevern et al. 2008). A prior study conducted on traditional pervious concrete found that a small replacement of coarse aggregate with sand (~7% by weight) increased the compressive strength of pervious concrete by 18% (Kevern et al. 2008). It has also been suggested that TiO_2 is capable of improving the mechanical strength of cement mortar. In their study, Chen, et al. (2012) reported that additions of 5 and 10% by weight of cement increased the 28-day strength of mortar by approximately 10-25%. This increase in strength has been attributed to a nano-filler effect through which the TiO_2 nanoparticles provide additional nucleation sites for cement hydration, thereby increasing both the rate and degree of hydration (Jayapalan, Jue, and Kurtis 2014). Therefore, this study analyzed the impact of both sand and TiO_2 additions on the mechanical, physical, and hydraulic properties of MPC. Finally, the suitability of the well-known Carman-Kozeny model to predict the permeability-porosity relationship of MPC was investigated herein.

Chapter 3 Research Methods and Materials

This research was performed in three (3) experimental phases. In the first phase, plain cement and TiO_2-cement blend mortar samples were formulated and cast to examine the impact of TiO_2 on compressive strength of cement-based mortars at 3-, 7- and 28-days. In the second phase, the RCA samples were characterized for composition, gradation, unit weight, specific gravity, and absorption. In the third phase, MPC cylinders were designed and cast to study the impact of RCA, sand, and TiO_2 on the mechanical, physical, and hydraulic properties of MPC.

3.1 Research Materials

Type I/II cement, virgin coarse aggregate (pea gravel), and sand was obtained from a local hardware store. RCA, which consisted of crushed mortar, reclaimed virgin aggregate, crushed masonry, and asphalt was acquired from Allied Recycled Aggregates in Commerce City, Colorado USA. Both virgin coarse aggregate and RCA were sieved to yield a uniform particle size of No. 4 (4.75 mm). Rutile TiO_2 with an average particle size of 0.41 µm was acquired from DuPont. MasterGlenium 3400 was used as a high-range water reducer.

3.2 Mortar Cube Preparation and Testing

Three (3) sets of six (6) mortar cube specimens were cast for each of five (5) sample formulations according to ASTM C109. Each set was used for 3-, 7-, and 28-day compressive strength tests. Table 1 shows the mix designs of the five (5) sample formulations. The Control sample was proportioned according to ASTM C109 for portland cement mortars. The remaining four mortar mixes were modified with binder additives (either cement, “C”, or TiO_2, “T”). The number (“2.5” or “5”) in the mix nomenclature indicates the percent addition of additional cement or TiO_2 by weight of cement. Given that both cement and TiO_2 additions were treated as binder components, a total water-to-binder (w/b) ratio is reported instead of a water-to-cement (w/c) ratio.

Table 1—Mix Design Proportions for Mortar Testing

Mix	Cement, lb [g]	Sand, lb [g]	Water, lb [g]	TiO_2, lb [g]	w/b
Control	1.10 [500]	3.03 [1375]	0.53 [242]	--	0.48
2.5C	1.13 [512.5]	3.03 [1375]	0.53 [242]	--	0.47
5C	1.16 [525]	3.03 [1375]	0.53 [242]	--	0.46
2.5T	1.10 [500]	3.03 [1375]	0.53 [242]	0.03 [12.5]	0.47
5T	1.10 [500]	3.03 [1375]	0.53 [242]	0.06 [25]	0.46

Since curing rooms simulate non-realistic conditions for pervious concrete curing, one was not utilized in this study. To simulate worst-case field conditions, mortar specimens were exposed to ambient air during curing. One additional set of Control specimens was cast and placed in a curing room in order to compare the ideal conditions to the simulated field conditions. This additional set of Control specimens was cured for a full 28 days prior to testing. Compressive testing of the mortar cubes was conducted using a 100-kip MTS load frame with a loading rate of 0.0006 in/s (0.015 mm/s). All specimens were loaded past the peak stress to observe post-peak behavior.

3.3 Recycled Aggregate Characterization

Along with the virgin coarse aggregate, the physical properties of three (3) candidate blends (A, B, C) of RCA were characterized. These blends were mixed by the RCA supplier and originally designed as different blends for aggregate road base. Blend A consisted of RCA with particle sizes of 1.5" (40 mm) or less. Blend B consisted of a well-graded aggregate blend that met Colorado Department of Transportation Class 6 classification. Class C consisted of concrete crusher fines.

The unit weight and gradation of the virgin and recycled aggregates (A, B, C) were measured using ASTM C29 and ASTM C136, respectively. After sieving of the blends, ASTM C29 was also used to measure the unit weight of the selected aggregate size, No. 4 (4.75 mm). The No. 4 (4.75 mm) aggregate of the most promising RCA blend and virgin aggregate was then tested for specific gravity and absorption according to ASTM C127. A simple composition analysis for the No. 4 (4.75 mm) of the selected RCA blend was carried out by visual inspection. A small sample of the aggregate was weighed and then each aggregate type within the sample (e.g. crushed mortar, reclaimed aggregate, asphalt) was segregated and individually weighed to obtain a percent-weight of each aggregate type. After characterization of the aggregate samples, the virgin aggregate and selected RCA blend was sieved to a uniformly graded No. 4 (4.75 mm) particle size for use in the MPC mixes.

3.4 Macroporous Pervious Concrete Cylinder Preparation and Testing

Seven (7) MPC sample formulations were designed and cast according to the mix design proportions presented in Table 2. The National Ready Mix Concrete Association (NRMCA) methodology was used to proportion the mixes. The control mix was the only mix to use virgin aggregate while the remaining mixes all contained RCA. "RCA" in the mix name indicates that only RCA coarse aggregate was put into the mix while "RCAs" indicates an addition of sand to the RCA. Sand was added as a 7% by weight replacement of the coarse aggregate. The TiO_2 was added as a percent addition by weight of cement. The number in the mix name indicates the percent addition of TiO_2. A high-range water reducer (HRWR) was added to each mix at a dosage of 2 oz./cwt (59 mL/cwt).

The MPC cylinders were mixed according to what the authors refer to as a slurry build-up method. In this method, the cement paste is built-up around the aggregate. The first step of the method combines all aggregates, coarse and fines, with a small percentage of the batched cement for thirty seconds. A fourth of the cement (and TiO_2, if applicable) and batch water was added and allowed to combine in the mixer for one minute. This was repeated until all cement and water was added. Upon the last addition of cement and water, the concrete was mixed for three minutes. Lastly, the concrete was allowed to rest for two minutes and then mixed for a final one minute. The TiO_2 was added in fourths and given time to mix in an effort to ensure an adequate dispersion of the particles. A proper dispersion of nanoparticles like TiO_2 is known to be important for maximizing the effectiveness of the particles' properties in the mix (Yousefi, Allahverdi, and Hejazi 2013).

To achieve high porosity to create MPC, light consolidation was used in the casting of cylinders. Even though rodding was found to be inferior to using a Proctor hammer (Putman and Neptune 2011), rodding was still preferred for casting MPC cylinders because it gave a higher probability of achieving the desired ultra-high porosity. Concrete was added in two lifts to 4" x 8" (100 mm x 200 mm) cylinder molds, with each lift being rodded five times. The rodding was applied equally across the area of the cylinder. This light rodding method is in contrast to the traditional consolidation method for pervious concrete found in ASTM C1688. The MPC was cured under simulated field conditions. To simulate field curing methods prescribed in the ACI Report 522.1-13, the cylinders were left in their molds for seven days while covered in plastic. After seven days, the cylinders were removed and left exposed to ambient indoor air conditions. This curing method was chosen in an attempt to best simulate field curing.

Table 2—Mix Design Proportions for Pervious Concrete Cylinder Testing

Mix	Water, lb/yd^3 [kg/m^3]	Cement, lb/yd^3 [kg/m^3]	Aggregate, lb/yd^3 [kg/m^3]	Sand, lb/yd^3 [kg/m^3]	TiO_2, lb/yd^3 [kg/m^3]
Control	222 [132]	823 [489]	2273 [1350]	--	--
RCA	184 [109]	683 [405]	2216 [1316]	--	--
RCAs	184 [109]	683 [405]	2071 [1230]	145 [86]	--
RCA+2.5	184 [109]	683 [405]	2216 [1316]	--	17 [10]
RCAs+2.5	184 [109]	683 [405]	2071 [1230]	145 [86]	17 [10]
RCA+5	184 [109]	683 [405]	2216 [1316]	--	34 [20]
RCAs+5	184 [109]	683 [405]	2071 [1230]	145 [86]	34 [20]

At 28 days, the cylinders were capped with a sulfur compound as per ASTM C617 and compressive testing was performed according to ASTM C39. Compression testing was load-controlled with an average rate of 30 psi/s (0.21 MPa/s). Moduli of elasticity were calculated by determining the slope of the stress-strain curves. The average unit weight, compressive strength, and modulus of elasticity were measured for each mix design. Porosity was determined for each mix according to a modified ASTM C1754. MPC cylinders were not oven dried and the air-dry mass was substituted for the oven-dry mass. At least three cylinders were used in the determination of average porosity. Permeability of the cylinders was determined with a falling-head permeameter as described in (Kevern et al. 2008). Three cylinders of each mix were measured for permeability with each cylinder being tested at three different initial head values.

A preliminary trial study of MPC cylinders was conducted for the RCA and RCAs blends. This study used the same mix design and casting methods as previously seen in Table 2 and described in this section. The only exception was that compaction was achieved by 5 seconds of vibration on a vibrating table in lieu of rodding. This trial study was carried out for the purpose of obtaining rough estimates of strength for the subsequent batches.

Chapter 4 Results

4.1 Mortar Cube Compressive Strength

A complete set of stress-strain curves for each sample of the five mortar formulations is given in Appendix A. The results in the appendix are summarized into strength development for the formulations. The development of the average 3-, 7-, and 28-day compressive strength for all mortar specimens is shown in Figure 1. Error bars in the figure represent standard deviations. The maximum compressive strength was achieved (or nearly achieved) by most of the mortars after 7 days of curing. For example, the difference between the control 7- and 28-day compressive strength was less than 0.1%. The impact of ambient-condition versus moisture-condition curing is also shown in Figure 1. The compressive strengths of the ambient- and moisture-cured samples were 4.83 ksi (33.3 MPa) and 5.18 ksi (35.7 MPa), respectively, which corresponds to a 7.3% gain in strength due to the ideal conditions of the moisture-curing process.

Comparing the 3-day compressive strengths for all formulations in Figure 1, the 2.5% and 5% addition of cement caused reductions in the 3-day compressive strength of the mortars by 3.5% and 0.9%, respectively, although this difference is small and not considered significant. The 2.5% and 5% addition of TiO_2, however, increased the 3-day compressive strengths of the control mortar by 9.1% and 5.2%, respectively. In comparing 28-day strengths, the 2.5% and 5% additions of cement or TiO_2 ameliorates the initial strength losses associated with the non-ideal curing conditions, suggesting that the binder additions improves the hydration of the cement paste.

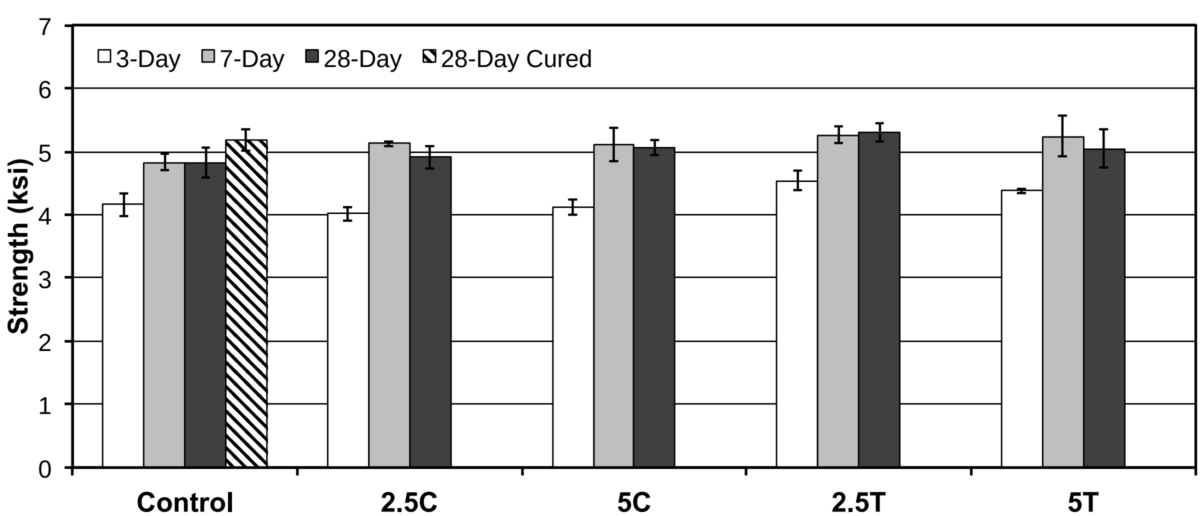

Figure 1—Strength Development of All Mortar Formulations [1 ksi = 6.9 MPa]

The relative percent changes from the 3-, 7-, and 28-day compressive strength of the control mortar are given in Table 3 for all sample formulations. At seven days, additions of both cement and TiO_2 contributed to approximately 6% and 8.5% increases in strength, respectively, suggesting that the TiO_2 additions are more effective for increasing strength at this age. There were no significant differences between the 2.5% and 5% additions for either cement or TiO_2. At 28 days, both the 2.5% and 5% cement additions had strength increases of less than 5% compared to the 28-day strength of the control mortar. While the 5% TiO_2 formulation also did not demonstrate any significant improvement in 28-day strength of the control mortar, the 2.5% TiO_2 formulation increased the compressive strength of the control specimen by 9.7%, which was a greater increase than the specimen cured in ideal moisture-curing conditions. The 9.7% increase in strength in the mortar specimens is similar to the increases in strength found by Chen, et al. (2012), for both 5% and 10% additions of anatase TiO_2. Both additions had relative strength gains of approximately 10% at 28 days. This suggests that both forms of TiO_2, rutile or anatase, is able to provide benefits in compressive strength and that 2.5% is the maximum addition needed to achieve strength gains. There was no added strength benefit at higher dosage levels.

To elucidate the effect of the TiO_2 additive on the compressive strength development of the control mortar, the 3- and 28-day compressive strengths are presented in terms of their w/b ratios in Figure 2 and Figure 3, respectively. In these figures, the w/b ratio of each formulation is plotted against average compressive strength. For the 28-day results, the strength of the cured specimen is also provided for comparison. The percentages indicate the difference of the modified formulation (with TiO_2 or curing) to the cement-only formulations. Figure 2 shows that there are significant increases in strength for the TiO_2-blend formulations in early-age conditions. The increases are not as large at 28 days (Figure 3). There is no improvement for a w/b of 0.46, and, in the case of a w/b of 0.47, the addition of TiO_2 increased the strength of the mortar more than curing it in ideal moisture conditions. As anticipated, these data suggest that the addition of TiO_2 enhances cement hydration and promotes early-strength development. These findings corroborate previous results reported by Jayapalan, et al. (2014).

Table 3—Relative Strength Increases for Mortar Samples

Mix	3-Day	7-Day	28-day
Control	0.0%	0.0%	0.0%
2.5C	-3.5%	6.0%	1.8%
5C	-0.9%	5.7%	4.8%
2.5T	9.1%	8.8%	9.7%
5T	5.2%	8.5%	4.4%
Cured	--	--	7.3%

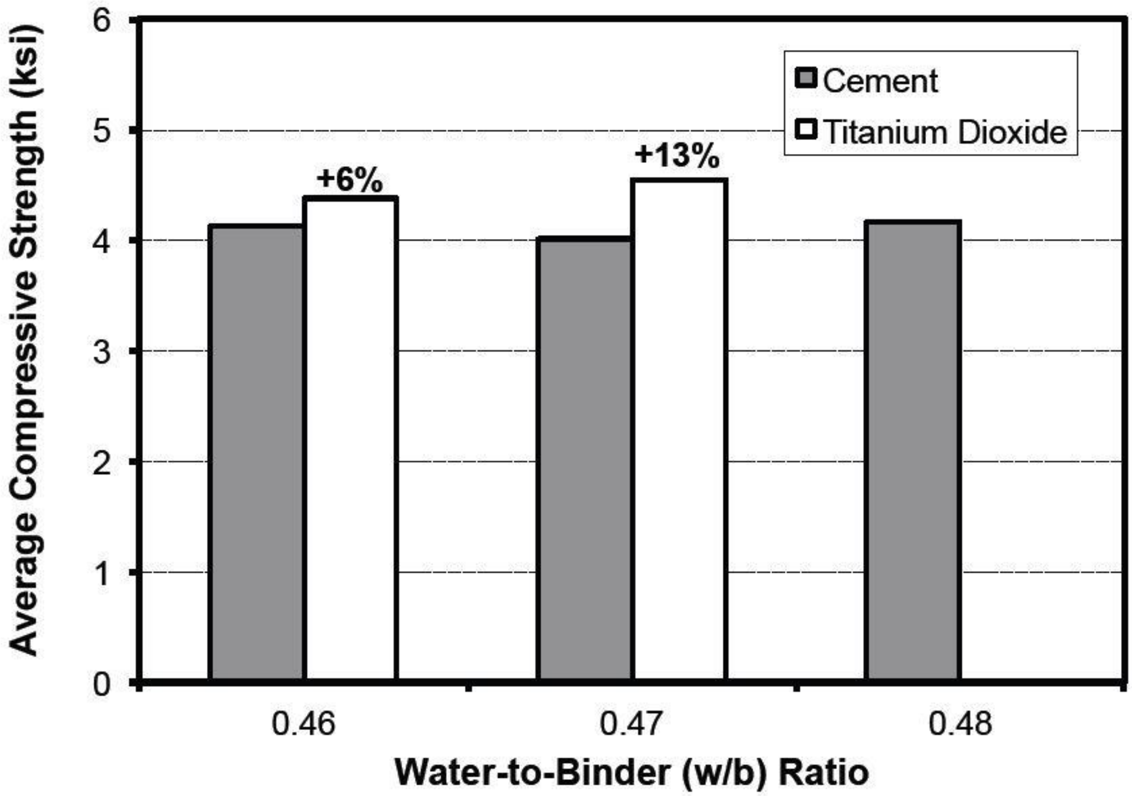

Figure 2—3-Day Strength Comparison for Samples with Equal Water-to-Binder Ratios [1 ksi = 6.9 MPa]

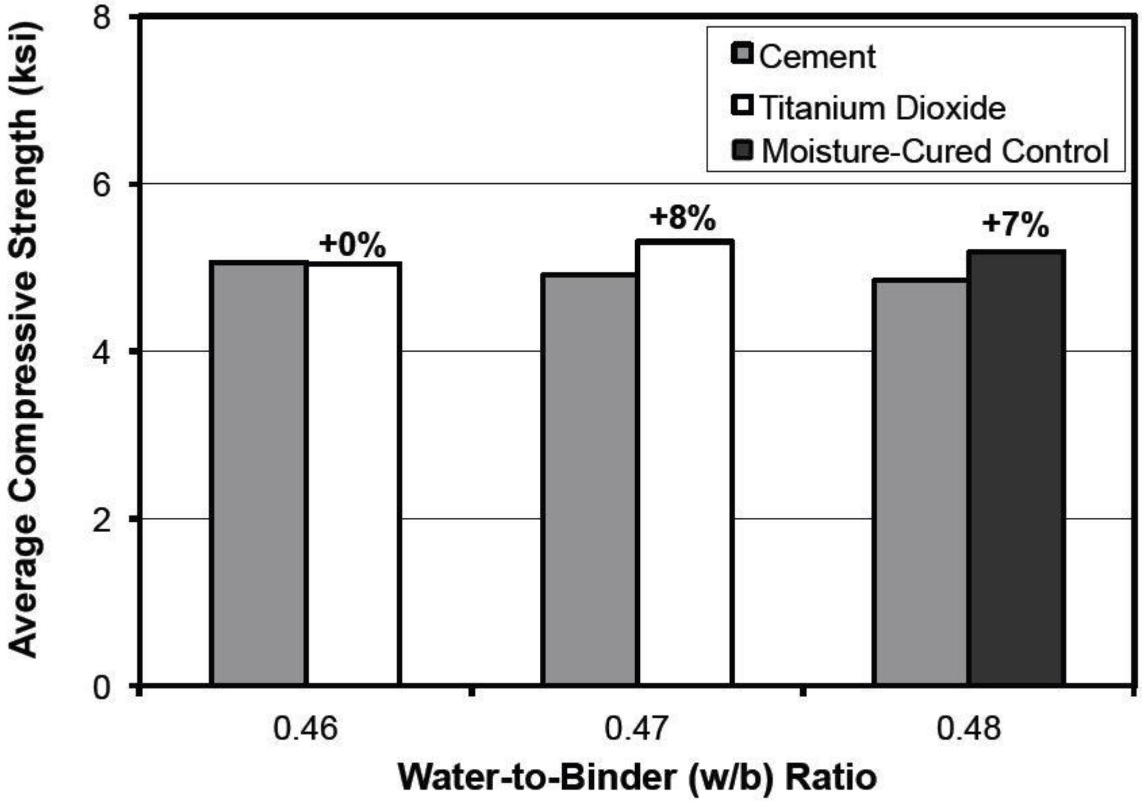

Figure 3—28-Day Strength Comparison for Samples with Equal Water-to-Binder Ratios [1 ksi = 6.9 MPa]

4.2 Recycled Aggregate Properties

The unit weight and gradation results for the three candidate RCA blends are given in Table 4. In lieu of complete gradation results, only the percent retained on the No. 4 (4.75 mm) sieve is reported, as it was the quantity of interest from the gradation analysis. The Class A blend had the largest unit weight but also the smallest amount of the desired aggregate size at 14.9% retained. The other blends, Class B and Class C, contained much more of the desired aggregate at 21.5 and 29.9%, respectively, retained on the No. 4 (4.75 mm) sieve. The unit weights of these two blends were also very similar at 98.4 lb/ft^3 (1580 kg/m^3) and 98.9 lb/ft^3 (1580 kg/m^3), respectively. Because of its lower amount of the chosen aggregate, the Class A blend was eliminated from further analysis.

Table 4—Raw RCA Characterization

RCA Blend	Unit Weight, lb/ft^3 [kg/m^3]	Percentage Retained on No. 4 [4.75 mm] Sieve
Class A	103.5 [1660]	14.9%
Class B	98.4 [1580]	21.5%
Class C	98.9 [1580]	29.9%

The Class B and Class C blends were sieved to obtain a sufficient amount of No. 4 (4.75 mm) for unit-weight characterization. As the unit weight results in Table 5 indicate, there was little difference between the aggregate from the different blends. This was also confirmed with a visual inspection of the sieved aggregate, as no appreciable difference was observed between the samples. Bulk specific gravity and absorption were then measured for the RCA. The RCA displayed properties that were noticeably different from the virgin aggregate. The bulk specific gravity of 2.16 was much lower than the virgin aggregate at 2.60 and the absorption of the RCA at 8.38% was higher than the absorption of the virgin aggregate at 1.11%. Both of these differences were expected because of the porous nature of the RCA compared to the virgin aggregate. However, these results indicate that RCA may not provide good freeze-thaw durability because of the high absorption and low specific gravity of the material (Vancura, MacDonald, and Khazanovich 2011). Class B and Class C RCA consisted mostly of crushed mortar, as can be seen in Table 6. Crushed mortar is more porous than the pea gravel, which would consequently increase the absorption of the material, as observed. The composition of the RCA is controlled by demolition projects that supply the raw material. This raw material may be masonry, asphalt, reclaimed coarse aggregate or crushed mortar of various strengths. While this inevitably leads to a high variability in composition and, subsequently, absorption of the RCA, an absorption of 8.38% as given in Table 5 was assumed for all RCA used in the study.

Table 5—No. 4 Aggregate Characterization

Aggregate Type		Unit Weight, lb/ft^3 [kg/m^3]	Bulk Specific Gravity	Absorption, %
RCA	Class B	83.3 [1330]	2.16	8.38%
	Class C	82.4 [1320]		
Virgin	Gravel	91.3 [1460]	2.60	1.11%

Table 6—Aggregate Composition

Constituent Material	Mass, lb [g]	Percent of Total
Mortar	0.12 [56]	87.5%
Asphalt	0.0022 [1]	1.6%
Reclaimed Aggregate	0.015 [7]	10.9%

4.3 Physical and Hydraulic Properties of Marcoporous Pervious Concrete

The average permeability and porosity of each MPC mix is presented in Figure 4. The error bars indicate the standard deviation of the permeability for each MPC sample formulation. All formulations had a permeability of approximately 2.50 in/s (6.3 cm/s) with the exception of RCA mix, which exhibited a permeability of 3.28 in/s (8.2 cm/s). This was anticipated given that the RCA mix also exhibited the highest porosity (see Figure 4). Also as expected, the addition of sand decreased the permeability of MPC when compared to the MPC mix with no sand (e.g., RCAs+5 vs. RCA+5). The magnitude of the permeability for all MPC samples was much higher when compared to typical pervious concrete values reported in ACI 522R-10. This was also expected because of the ultra-high porosity of MPC. The porosity ranged from a low of 35% for the Control and RCAs mixes to a high of 42% for the RCA mix. The remaining mixes all had a porosity of approximately 38%. All of these porosities are greater than 30%, which classifies them as MPC as defined by the authors herein.

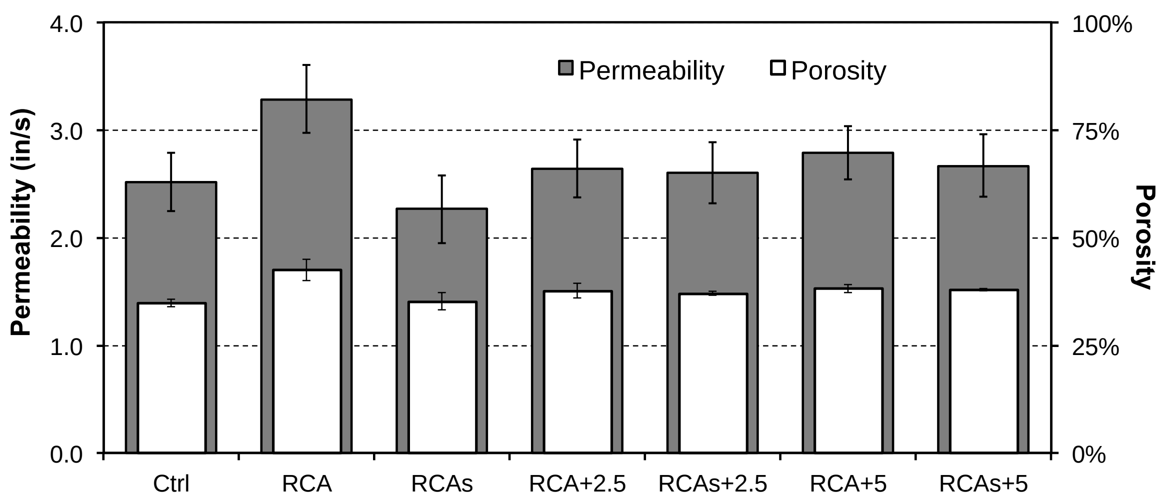

Figure 4—Comparison of MPC Cylinder Permeability [1 in/s = 2.5 cm/s]

4.4 Mechanical Properties of Macroporous Pervious Concrete

During mixing of the MPC samples, the impact of the TiO_2 additions could be easily observed. For both 2.5% additions, the MPC became viscid with large volumes of the material forming a large cake in the bottom of the mixer. This large cake was easily broken apart with a scoop, but it remained solid if left undisturbed. For the 5% additions, the MPC was highly viscid, to the point where it stuck to itself and the mixer was nearly clean after the concrete was removed. These results seem to agree with a previous study on the impact of TiO_2 on the rheology of cement mortars conducted by Senff, et al. (2012), who reported that the addition of TiO_2 to cement mortars increased the torque and yield stress while decreasing the spread on table. These results could be explained by the TiO_2 giving the mortar a viscid nature as was observed in this study.

The 28-day compressive strengths for all seven (7) MPC mix designs are shown in Table 7. As expected, the compressive strengths are low in magnitude compared to traditional concrete or typical pervious concrete due to the ultra-high porosity of MPC. In a comparison of virgin aggregate (Control) and RCA MPC samples, the data in Table 7 indicate that the use of recycled aggregates is not detrimental to the MPC compressive strength. This implies that the binder (which is varied in the other MPC mixes), not the aggregate, controls the mechanical properties of MPC. The ability to incorporate RCA without a compromise in material properties has positive economic and environmental implications. A broadened application of MPC presents a new opportunity to reuse construction waste in novel means and divert the waste from landfills, while reducing the economic and environmental costs associated with the mining and transport of virgin aggregates.

Table 7 also shows that a 7% addition of sand (RCAs) increased the strength of MPC and that these relative strengths were higher than the best-performing TiO_2 addition (RCA+2.5). This suggests that sand was more effective at increasing compressive strength than TiO_2 when used individually. However, when both sand and TiO_2 were added to the paste (RCAs+2.5), the MPC displayed a relative strength increase of 28% compared to the control mix, suggesting a synergistic interaction between both additives. Furthermore, a 2.5% addition of TiO_2 increased the strength of MPC cylinders by 7%, whereas an addition of 5% TiO_2 was detrimental to the compressive strength of the MPC cylinders. This pattern is similar to the results of the mortar samples where the 2.5% addition of TiO_2 gave strength benefits while the 5% addition gave no change compared to the control (see Table 3). The compressive strength of MPC also decreased with the addition of 5% TiO_2 and sand (RCAs+5).

The use of sand or TiO_2 as a means to increase the binder strength of MPC is important because as stated previously, the binder strength controls the MPC strength. If the strength were increased enough, MPC could potentially be used as a pavement or another type of horizontal infrastructure. A MPC pavement would be of interest because the large porosity of the material could help reduce the costs of maintenance by reducing clogging. The ACI 522R-10 document reports that clogging is a significant issue for pervious concrete. The large porosity of MPC could reduce clogging by allowing sediment and debris to flow through the material instead of catching it.

The modulus of elasticity for each MPC mix, along with the relative increases in stiffness for each mix (compared to the control), is shown in Table 8. Similar to the compressive strength results in Table 7, there was little difference between the virgin aggregate Control and the RCA sample. RCAs demonstrates that the addition of sand (7%) increased the modulus of elasticity of MPC by 19%. Both the 2.5% and 5% additions of TiO_2 decreased the modulus of elasticity by 7% and 4%, respectively. When sand is added to the 2.5% TiO_2 addition (RCAs+2.5), the modulus of elasticity increases by 28%. This trend is not valid for the 5% addition of TiO_2 (RCAs+5), where the addition of sand further decreased the modulus of elasticity. This reduction in modulus is similar to the reduction in compressive strength shown in Table 7.

Table 7—Strength Comparison for MPC Cylinders

Mix	Strength, psi [MPa]	Relative Strength
Control	456 ± 38 [3.1 ± 0.26]	--
RCA	458 ± 31 [3.2 ± 0.22]	1.00
RCAs	542 ± 76 [3.7 ± 0.52]	1.19
RCA+2.5	488 ± 53 [3.4 ± 0.37]	1.07
RCAs+2.5	584 ± 35 [4.0 ± 0.24]	1.28
RCA+5	404 ± 10 [2.8 ± 0.07]	0.89
RCAs+5	306 ± 30 [2.1 ± 0.21]	0.67

Table 8—Modulus of Elasticity Comparison for MPC Cylinders

Mix	Modulus of Elasticity, psi [GPa]	Relative Modulus of Elasticity
Control	244,560 ± 29,350 [1.69 ± 0.20]	--
RCA	249,360 ± 24,880 [1.72 ± 0.17]	1.02
RCAs	284,400 ± 51,290 [1.96 ± 0.35]	1.16
RCA+2.5	228,240 ± 32,520 [1.57 ± 0.22]	0.93
RCAs+2.5	258,800 ± 29,010 [1.78 ± 0.20]	1.06
RCA+5	236,000 ± 5,660 [1.63 ± 0.04]	0.96
RCAs+5	217,870 ± 21,090 [1.50 ± 0.15]	0.89

The 5% addition of TiO_2 provided little benefit to the mortar samples and being detrimental to the compressive strength and modulus of elasticity of the MPC cylinders. Even though this result was not anticipated, the loss in favorable mechanical properties may be attributable to two possible mechanisms related to the field curing methods. The first possible mechanism is the photochemical reactions that occur with TiO_2. Along with the removal of pollutants through a redox reaction, TiO_2 becomes hydrophilic in the presence of UV radiation. This hydrophilicity has been noted by multiple authors (Chen and Poon 2009; Diamanti, Ormellese, and Pedeferri 2008). The difference in curing location, between the environmental chamber used in a study by Chen, et al. (2012) and the exposed laboratory space used in this study, could result in different amounts of UV exposure. The light sources in the exposed laboratory space of this study could have provided UV radiation to both the mortar and MPC throughout the curing process. Thus, the TiO_2 in the samples could have become hydrophilic and bound water that was not available for complete or thorough cement hydration. This process would explain why the 5% TiO_2 additions did not suffer early age strength losses as seen in Figure 1 and Table 3. At three days, significant time had not yet passed which would prevent sufficient UV radiation from photo-inducing hydrophilicity in the TiO_2. However, after 28 days of exposure to UV radiation, the TiO_2 may have become hydrophilic. The second possible mechanism is autogenous shrinkage. In a study done by Jayapalan (2013), the replacement of cement with TiO_2 in cement-based materials was found to increase autogenous shrinkage. Smaller TiO_2 particle sizes resulted in more shrinkage. The autogenous shrinkage was caused by the fine TiO_2 particles giving a smaller inter-particle spacing within the paste which can increase capillary stress (Jayapalan 2013). This is similar to the autogenous shrinkage found in the supplementary cementitious material, silica fume (Bhuvaneshwari and Sasmal 2012). The shrinkage behavior of the TiO_2 was possibly exacerbated by the simulated field curing methods. In the ambient conditions, water was able to evaporate into the environment which could in turn further increase capillary stress. Thus, the 5% addition did not perform as well as the 2.5% addition. These phenomena could also explain why the loss of mechanical properties was greater in the MPC cylinders than the mortar specimens. With a much larger exposed surface area, more TiO_2 could be exposed to UV radiation or contribute to additional autogenous shrinkage, leading to a lower degree of hydration or excess internal stresses. The autogenous shrinkage mechanism is more likely as the specimens were not subjected to direct UV radiation. Therefore, an addition limit of 2.5% by weight of cement for TiO_2 is recommended due to its ability to enhance hydration by providing additional nucleation sites while not being a large enough quantity for the simulated field conditions to detract from cement hydration.

4.5 Macroporous Pervious Concrete Property Relationships

The relationship between the modulus of elasticity and unit weight for all MPC cylinders is presented in Figure 3. It can be seen that the modulus of elasticity remains relatively constant across the entire range of unit weight values, which indicates that the modulus of elasticity is independent of unit weight for MPC.

The relationship between the 28-day compressive strength and unit weight for all MPC cylinders is given in Figure 4. These data are appended to the existing data presented by ACI 522R-10 (from Mulligan 2005). Figure 4 shows that the unit weight of all MPC cylinders is lower than the range of unit weights previously recorded in ACI 522R-10. The ACI data does not extend below 105 lb/ft^3 (1680 kg/m^3), whereas the MPC in this study ranges from 83 to 98 lb/ft^3 (1330 to 1570 kg/m^3). Additionally, the compressive strengths of MPC are consistent, albeit lower, than the strengths reported by ACI. This indicates that for MPC, the compressive strength is independent of the unit weight and that a strength plateau exists around 500 psi (3.4 MPa) for the overall compressive strength versus unit weight relationship for pervious concrete.

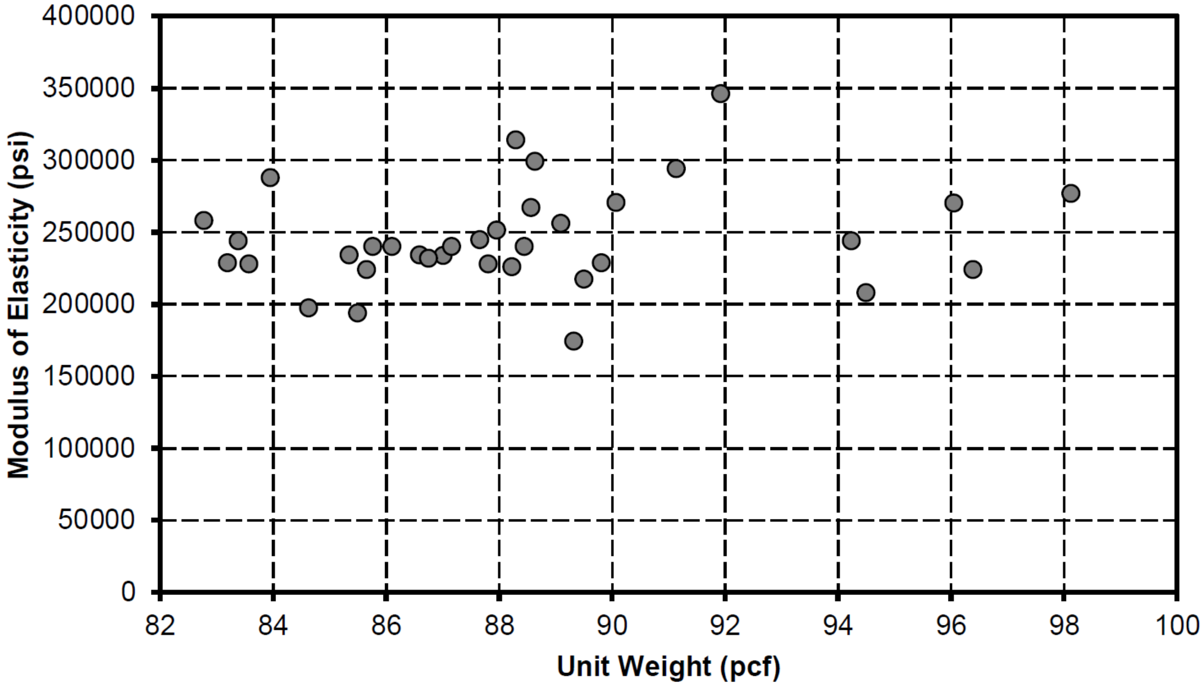

Figure 3—Relationship of Macroporous Pervious Concrete Modulus of Elasticity and Unit Weight [1000 psi = 6.9 MPa; 1 pcf = 16.0 kg/m^3]

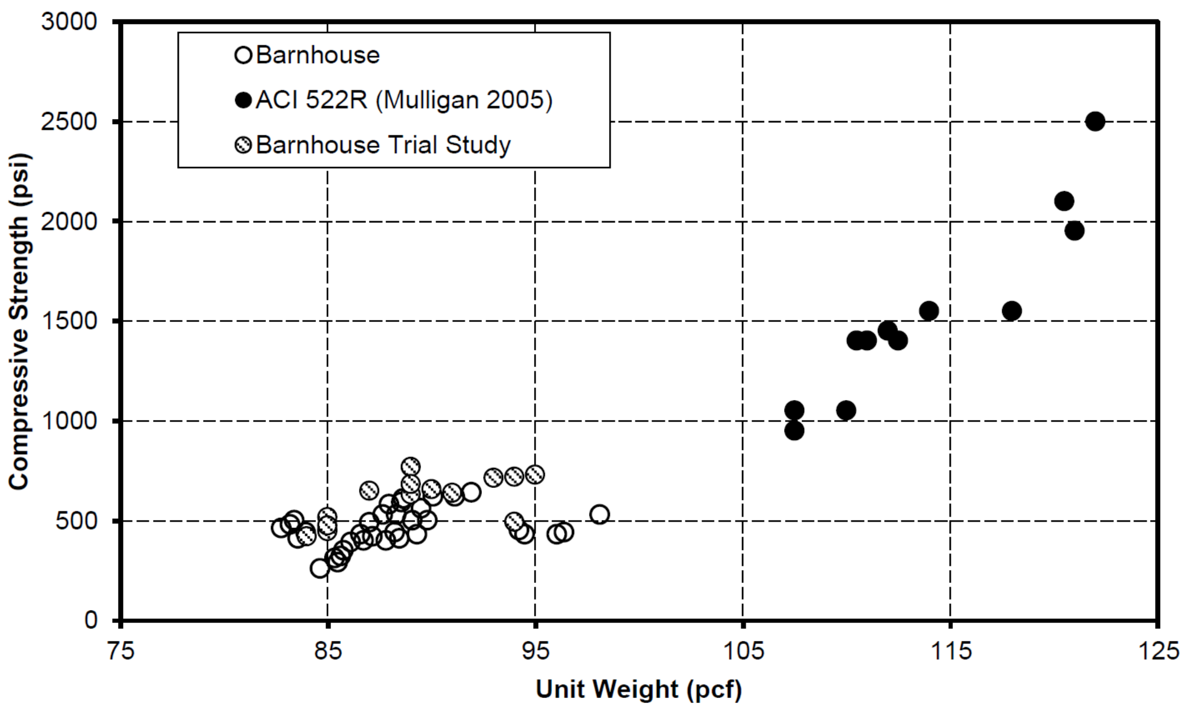

Figure 4—Relationship between Compressive Strength and Unit Weight for Conventional and Macroporous Pervious Concrete [1000 psi = 6.9 MPa; 1 pcf = 16.0 kg/m^3]

The relationship between average compressive strength and porosity for each MPC mix design is given in Figure 5. These data are also appended to data reported by ACI 522R-10 (from Meininger 1988). This study contributes previously unreported MPC data for porosities from 35% to 42%. A broad range of both compressive strength and porosity was found in the present study, while the range of compressive strengths was relatively narrow. For example, the unit weights in Figure 4 varied from 83 to 98 lb/ft^3 (1330 to 1570 kg/m^3) – a difference of 13 lb/ft^3 (208 kg/m^3) – while the compressive strengths ranged from 260 to 768 psi (1.8 to 5.3 MPa) – a difference of 508 psi (3.5 MPa). It is clear that an increase in unit weight corresponds to an increase in compressive strength for normal pervious concrete (<30% porosity) but this is not necessarily true for MPC. A similar trend of a narrower compressive strength range is seen in the influence of porosity in Figure 5. The narrow ranges of compressive strength in both relationships given in this study indicate that neither unit weight nor porosity is as important to MPC design as it is to the typical hydraulic design of pervious concrete for horizontal infrastructure.

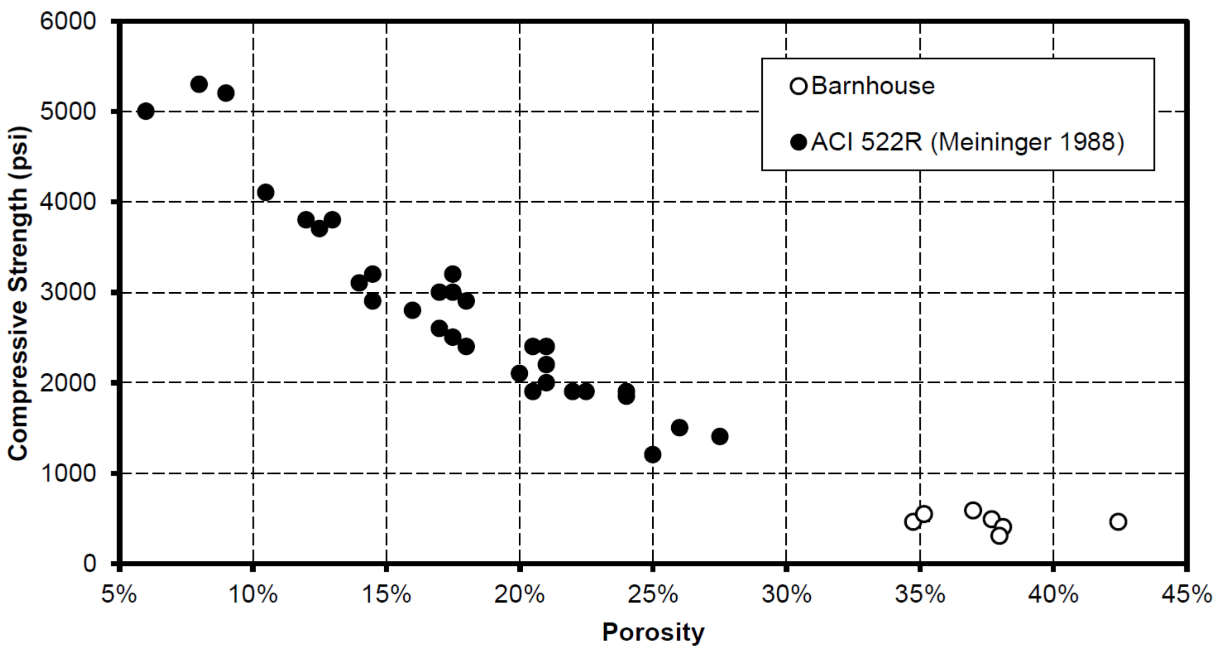

Figure 5—Relationship between Compressive Strength and Porosity of Conventional and Macroporous Pervious Concrete [1000 psi = 6.9 MPa]

The relationship between permeability and porosity of the MPC cylinders is shown in Figure 6. Similarly, the MPC data is added to data from the ACI 522R-10 (from Meininger 1988). Current ACI data contain some MPC data with porosities that range up to 35%. This research provides additional MPC data for porosities above 35%. Figure 6 shows that the permeability of the results in this study is higher than the permeability normal pervious concrete. This is also true for existing data with porosities of 35%. However, a range of permeability for a given porosity is not unprecedented, even within the existing data. For example, at an approximate porosity of 28%, the data give a permeability range from less than 1.0 cm/s (0.39 in/s) to greater than 2.0 cm/s (0.79 in/s).

Figure 6 also shows the conventional Carman-Kozeny predictive model, which is commonly used to predict the relationship between permeability and porosity of pervious concrete as described in Section 2.2. An α value of 30, as used by Kevern and Schaefer (2013) is able to accurately model the majority of the existing data. However, the existing data begin to deviate from the model at 30% porosity (the limit for MPC) and underestimates permeability. An α value of 45 more accurately models the data given by this research and the existing data above 30% porosity. The suitability of this value is also limited because it overestimates permeability below 30% porosity. Neither model seems valid for the entire range of pervious concrete data (10% to 45%). Therefore, a modified Carman-Kozeny equation is proposed and given in Equation 3. The proposed relationship is similar to the Carman-Kozeny relationship found in Equation 1. The difference is that the quantity in the denominator of the equation is cubed instead of squared. This modification adjusts the curvature of the equation and allows the equation to better fit the entire range of pervious concrete data. This equation is plotted over the data in Figure 7. The modified equation still contains some inaccuracies. It can be seen in Figure 7 that permeability is slightly over-predicted for pervious concretes with a porosity of approximately 20-30%. However, this inaccuracy is no worse than the inaccuracy of the unmodified models. This is shown in Figure 8. Figure 8 compares the experimental permeability results of this study and ACI 522R-10 to the calculated permeability of the original and modified Carman-Kozeny equations. A line of calculated permeability being equal to experimental permeability is plotted to provide a check of how close the calculated value is to the experimental value. The closer the datum point is to the line, the more accurate the calculation. If an equation over-predicts the permeability, the datum will fall above the line and the datum will fall below the line if permeability is under-predicted. It can be seen that both versions of the equation are fairly accurate and comparable to each other for a permeability of less than 4.0 cm/s (1.6 in/s). Above this point, the original Carman-Kozeny tends to under-predict the permeability of pervious concrete while the modified version is closer to the correct value with some data points falling on the line. This indicates that the modified equation is a better model for predicting pervious concrete permeability across the entire range of porosity. The modification of the Carman-

Kozeny equation may be necessitated because of a change in flow properties. The Carman-Kozeny equation assumes laminar fluid flow which may not be valid for MPC.

$$K = \alpha\left[\frac{p^3}{(1-p)^3}\right] \qquad \text{(Eqn. 3)}$$

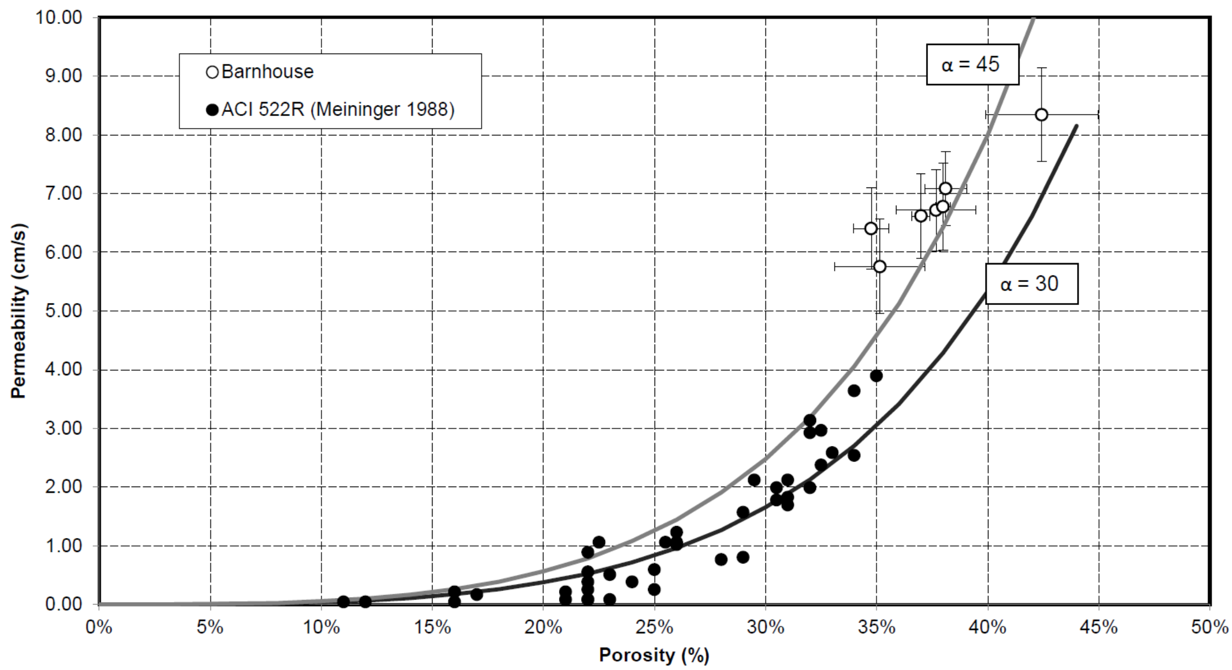

Figure 6—Empirical and Theoretical Relationship of Permeability and Porosity for Conventional and Macroporous Pervious Concrete as Predicted by the Carman-Kozeny Equation [2.5 cm/s = 1 in/s]

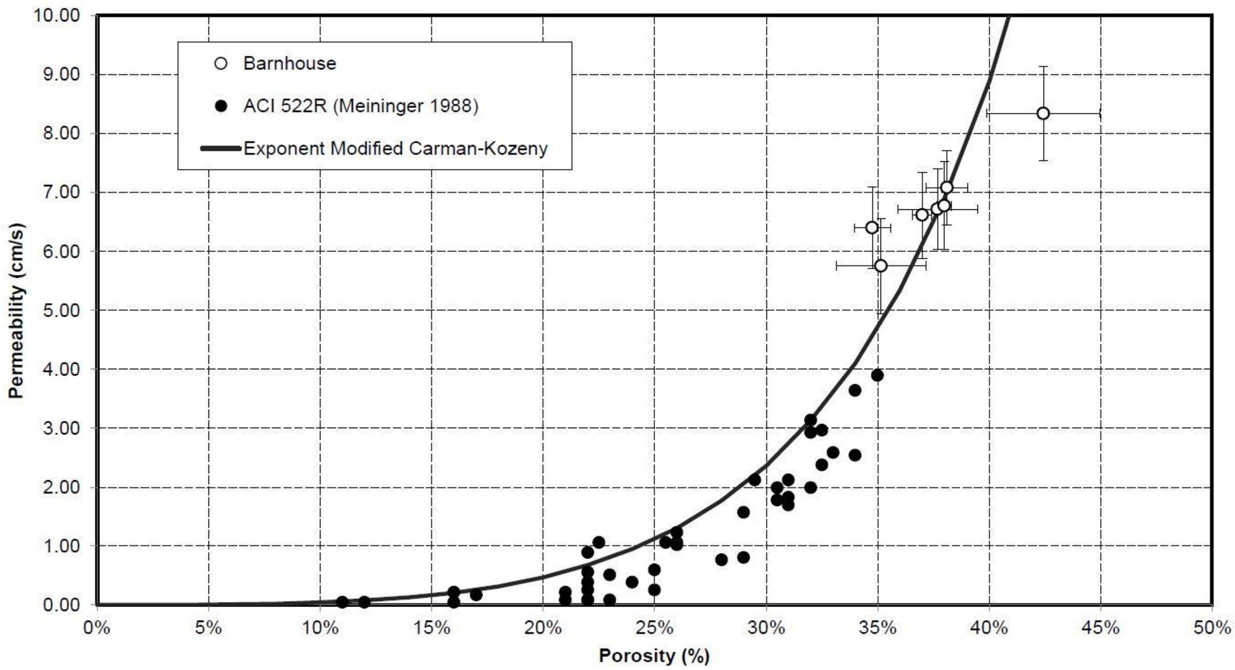

Figure 7—Proposed Relationship of Permeability and Porosity for Conventional and Macroporous Pervious Concrete Using a Modified Carman-Kozeny Equation [2.5 cm/s = 1 in/s]

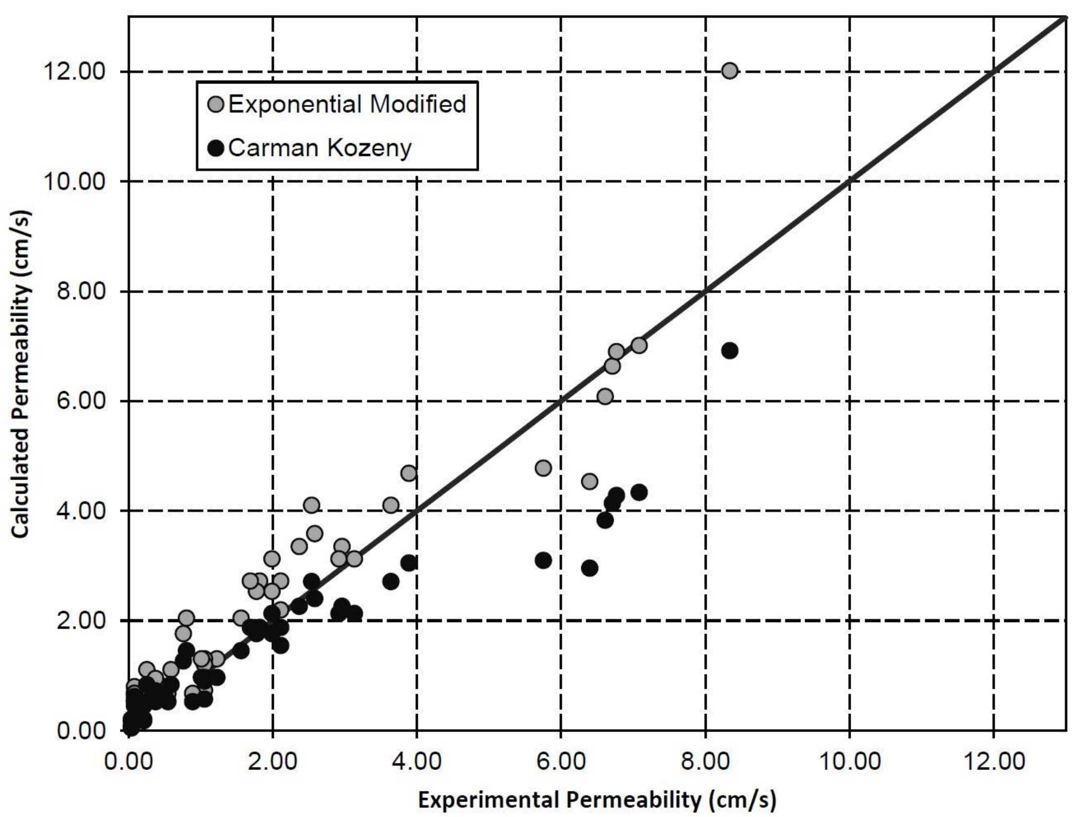

Figure 8—Comparison of Calculated Theoretical Permeability and Experimental Permeability Results for Conventional and Macroporous Pervious Concrete [2.5 cm/s = 1 in/s]

4.6 Sustainability Potential of Macroporous Pervious Concrete

Based on this study, MPC has the potential to be a highly sustainable building material for several advantageous reasons. First, MPC made with 100% RCA did not exhibit any decrease in compressive strength compared to the virgin-aggregate MPC. This is highly atypical, given that the replacement of virgin aggregate with recycled aggregate is well known to reduce the strength of standard pervious concrete (Berry et al. 2012; Gaedicke, Marines, and Miankodila 2014; Rizvi et al. 2010). The utilization of RCA conserves natural resources and decreases the volume of construction and demolition waste that is disposed into landfills. Second, the inclusion of TiO_2 to MPC mix design could contribute to the long-term environmental sustainability of urban environments. This study demonstrated that TiO_2 not only adds strength to MPC, which could increase MPC durability and service-life, but TiO_2 also removes pollutants through its photocatalytic activity (Asadi et al. 2012; Shen et al. 2012). Compared to conventional pervious concrete, MPC demonstrates an even higher possibility for the effectiveness of TiO_2 pollutant removal, given that its high porosity provides increased surface area over which the photo-initiated redox reactions can occur.

Chapter 5 Conclusions and Future Research

5.1 Conclusions

As of late, the use of pervious concrete with porosities up to 30% has increased in horizontal infrastructure applications because of its hydrologic and urban benefits. This increase in use has been due in large part to a greater improvement of design methodologies and a better understanding of the control of its mechanical and physical properties. Recently, there has been increased interest in new applications and potential uses for pervious concrete beyond horizontal infrastructure. Some of these applications will favor enhanced acoustic, thermal, or physical (e.g. porosity) properties over mechanical properties. Regardless of the growing interest in such applications, there has currently been little intentional research on the type of pervious concrete these applications demand. This research sought to characterize such a type of pervious concrete by investigating the physical, mechanical and sustainable properties of pervious concretes with porosities greater than 30%, defined in the present research as macroporous pervious concrete (MPC).

Mortar compression tests were an effective proxy to study the cement paste of MPC. Small additions of TiO_2 were found to enhance the rate and degree of cement hydration. The tests demonstrated that a 2.5% addition of titanium dioxide (TiO_2) increased the strength of the mortar by 9.7% in ambient, simulated field conditions and that benefits diminished at higher TiO_2 dosage levels. The 2.5% TiO_2 addition also gave results comparable to control samples moisture-cured under ideal conditions. Recycled concrete aggregate (RCA) blends were variable in composition but consisted predominantly of crushed mortar. This aggregate type may not provide sufficient freeze-thaw durability but carrying out tests to confirm this assumption was beyond the scope of work for this research.

In MPC mechanical testing, it was found that substituting virgin aggregates with recycled aggregates did not compromise compressive strength or impact the modulus of elasticity. Additionally, MPC is atypical when compared to conventional pervious concrete because it does not follow the existing material property relationships given by ACI. Neither porosity nor unit weight were key factors in determining compressive strength as they are for conventional pervious concrete. These results propose that the strength of MPC is dependent solely on the strength of the binder. A continuous Carman-Kozeny equation was not able to predict the permeability of entire range of both conventional and macroporous pervious concrete. Therefore, a piecewise Carman-Kozeny equation is proposed with different empirical coefficients for conventional and macroporous pervious concrete. The 2.5% addition of TiO_2 and 7% addition of sand to the MPC binder increased the concrete compressive strength by 7% and 19%, respectively. The same additions of binder additives gave a respective decrease in modulus of elasticity of 7% and an increase of 16%. Together, the 2.5% TiO_2 and 7% sand additions increased the compressive strength of MPC by 28% while raising the modulus of elasticity by 6%. The results of the 5% addition of TiO_2 for both the mortar compressive tests and MPC mechanical tests stress the importance of performing field-simulated testing for TiO_2-cement blend materials so as to capture the impact of UV radiation. Overall, the results of this study indicate that recycled-aggregate MPC modified with small additions of photocatalytic TiO_2 and sand has the potential to be a sustainable material solution for applications where ultra-high porosities are required.

5.2 Future Research

This research represents some of the first work carried out to explicitly characterize the physical and mechanical properties of MPC. Additional mechanical and physical testing such tensile strength testing, freeze-thaw durability or abrasion resistance are areas of need. Another area of interest would be casting MPC samples in a slab, as in the field, to observe if laboratory cylinders are truly representative of properties in the field. Understanding the impact of supplementary cementitious materials on MPC could be beneficial. This could be one possible way to improve the binder strength of MPC, a research area of high importance as an increase in binder strength directly leads to an increase in MPC strength. An investigation of internal curing of MPC samples could also lead to improved strength and possibly offset strength losses from field curing and large amounts of TiO_2 additions.

In light of the current research, more effort should focus on the mechanical impacts of TiO_2 on normal pervious concrete. There would be benefit in knowing if the results found herein translate to pervious concrete with less than 30% porosity as well. Another area for further research is the rheological effects of TiO_2 additions on pervious concrete. As noted in Section 4.4, there was a clear rheological impact due to the TiO_2 but it was not analyzed in depth. Furthermore, it would be beneficial to test yet even lower doses of TiO_2 in an effort to find the minimum required addition to gain benefits. Lastly, it is advised that all future research involving TiO_2-cement blend materials be tested under simulated field conditions to capture the effect of environmental mechanisms, be it UV radiation, autogenous shrinkage or other deterioration mechanisms, that are known to affect the initial- and long-term performance of pervious concrete.

References

American Concrete Institute (ACI). 2010. “ACI 522.1-13—Specification for Pervious Concrete Pavement.” Farmington Hills, MI.

American Concrete Institute (ACI). 2013. “ACI 522.R-10—Report on Pervious Concrete.” Farmington Hills, MI.

American Society of Testing and Materials (ASTM). 2009. “C29/C29M—Standard Test Method for Bulk Density (‘Unit Weight’) and Voids in Aggregate.” West Conshohocken, PA: ASTM International.

American Society of Testing and Materials (ASTM). 2014. “ASTM C39/C39M—Standard Test Method for Compressive Strength of Cylindrical Concrete Specimens.” West Conshohocken, PA: ASTM International.

American Society of Testing and Materials (ASTM). 2013. “C109/C109M—Standard Test Method for Compressive Strength of Hydraulic Cement Mortars.” West Conshohocken, PA: ASTM International.

American Society of Testing and Materials (ASTM). 2015. “C127/C127M—Standard Test Method for Relative Density (Specific Gravity) and Absorption of Coarse Aggregate.” West Conshohocken, PA: ASTM International.

American Society of Testing and Materials (ASTM). 2014. “C136/C136M—Standard Test Method for Sieve Analysis of Fine and Coarse Aggregates.” West Conshohocken, PA: ASTM International.

American Society of Testing and Materials (ASTM). 2012. “C617/C617M—Standard Practice for Capping Cylindrical Concrete Specimens.” West Conshohocken, PA: ASTM International.

American Society of Testing and Materials (ASTM). 2003. “C666/C666M—Standard Test Method for Resistance of Concrete to Rapid Freezing and Thawing.” West Conshohocken, PA: ASTM International.

American Society of Testing and Materials (ASTM). 2014. “C1688/C1688M—Standard Test Method for Density and Void Content of Freshly Mixed Pervious Concrete.” West Conshohocken, PA: ASTM International.

American Society of Testing and Materials (ASTM). 2009. “C1701/C1701M—Standard Test Method for Infiltration Rate of In Place Pervious Concrete.” West Conshohocken, PA: ASTM International.

American Society of Testing and Materials (ASTM). 2013. “C1747/C1747M—Standard Test Method for Determining Potential Resistance to Degradation of Pervious Concrete by Impact and Abrasion.” West Conshohocken, PA: ASTM International.

American Society of Testing and Materials (ASTM). 2012. “C1754/C1754M—Standard Test Method for Density and Void Content of Hardened Pervious Concrete.” West Conshohocken, PA: ASTM International.

Asadi, Somayeh, Marwa M. Hassan, John T. Kevern, and Tyson D. Rupnow. 2012. “Development of Photocatalytic Pervious Concrete Pavement for Air and Storm Water Improvements.” *Transportation Research Record* 2290: 161–67. doi:10.3141/2290-21.

Ballari, M. M., M. Hunger, G. Hüsken, and H. J H Brouwers. 2010. “NOx Photocatalytic Degradation Employing Concrete Pavement Containing Titanium Dioxide.” *Applied Catalysis B: Environmental* 95: 245–54. doi:10.1016/j.apcatb.2010.01.002.

Bayles, Gary A., George E. Klinzing, and Shiao-Hung Chiang. 1989. “Fractal Mathematics Applied to Flow in Porous Systems.” *Particle & Particle Systems Characterization* 6 (1-4): 168–75. http://onlinelibrary.wiley.com/doi/10.1002/ppsc.19890060128/abstract.

Berry, B. M., M. J. Suozzo, I. a. Anderson, and M. M. Dewoolkar. 2012. “Properties of Pervious Concrete Incorporating Recycled Concrete Aggregate.” In *Transportation Research Board Annual Meeting*. http://www.uvm.edu/~transctr/research/grad/12-3994.pdf.

Bhuvaneshwari, B, and Saptarshi Sasmal. 2012. “Role of Nano Oxides for Improving Cementitious Building Materials.” *Journal of Civil …*, no. 2: 52–58. http://www.academicpub.org/jces/paperInfo.aspx?paperid=963.

Carsana, M., F. Tittarelli, and L. Bertolini. 2013. “Use of No-Fines Concrete as a Building Material: Strength, Durability Properties and Corrosion Protection of Embedded Steel.” *Cement and Concrete Research* 48. Elsevier Ltd: 64–73. doi:10.1016/j.cemconres.2013.02.006.

Chen, Jun, Shi Cong Kou, and Chi Sun Poon. 2012. “Hydration and Properties of Nano-TiO2 Blended Cement Composites.” *Cement and Concrete Composites* 34 (5). Elsevier Ltd: 642–49. doi:10.1016/j.cemconcomp.2012.02.009.

Chen, Jun, and Chi Sun Poon. 2009. “Photocatalytic Construction and Building Materials: From Fundamentals to Applications.” *Building and Environment* 44 (9). Elsevier Ltd: 1899–1906. doi:10.1016/j.buildenv.2009.01.002.

Crouch, L. K., Jordan Pitt, and Ryan Hewitt. 2007. “Aggregate Effects on Pervious Portland Cement Concrete Static Modulus of Elasticity.” *Journal of Materials in Civil Engineering* 19 (July): 561–68. doi:10.1061/(ASCE)0899-1561(2007)19:7(561).

Diamanti, Maria Vittoria, Marco Ormellese, and MariaPia Pedeferri. 2008. “Characterization of Photocatalytic and Superhydrophilic Properties of Mortars Containing Titanium Dioxide.” *Cement and Concrete Research* 38. Elsevier Ltd: 1349–53. doi:10.1016/j.cemconres.2008.07.003.

Federal Highway Administration (FHWA), State of the Practice National Review, Transportation Applications of Recycled Concrete Aggregate, 2004, 47 pp.

Gaedicke, C, A Marines, and F Miankodila. 2014. “A Method for Comparing Cores and Cast Cylinders in Virgin and Recycled Aggregate Pervious Concrete.” *Construction and Building Materials* 52: 49–503. http://www.sciencedirect.com/science/article/pii/S0950061813010751.

Ghafoori, Nader, and Shivaji Dutta. 1995. “Building and Nonpavement Applications of No-Fines Concrete.” *Journal of Materials in Civil Engineering* 7 (4): 286–89.

Goel, P. K. 2006. *Water Pollution-Causes, Effects and Control*. New Delhi: New Age International.

Haselbach, Liv. 2009. “Pervious Concrete and Mitigation of the Urban Heat Island Effect.” In *Transportation Research Board 88th Annual Meeting*.

Haselbach, Liv, M. Boyer, J. T. Kevern, and V. R. Schaefer. 2011. “Cyclic Heat Island Impacts on Traditional Versus Pervious Concrete Pavement Systems.” *Transportation Research Record* 2240: 107–15.

Hüsken, G., M. Hunger, and H. J H Brouwers. 2009. “Experimental Study of Photocatalytic Concrete Products for Air Purification.” *Building and Environment* 44 (12). Elsevier Ltd: 2463–74. doi:10.1016/j.buildenv.2009.04.010.

Jang, J.G., Y.B. Ahn, H. Souri, and H.K. Lee. 2015. “A Novel Eco-Friendly Porous Concrete Fabricated with Coal Ash and Geopolymeric Binder: Heavy Metal Leaching Characteristics and Compressive Strength.” *Construction and Building Materials* 79. Elsevier Ltd: 173–81. doi:10.1016/j.conbuildmat.2015.01.058.

Jayapalan, Amal R., Melinda L. Jue, and Kimberly E. Kurtis. 2014. "Nanoparticles and Apparent Activation Energy of Portland Cement." *Journal of the American Ceramic Society* 97: 1534–42. doi:10.1111/jace.12878.

Jayapalan, Amal Raj Puthur. 2013. "Properties of Cement-Based Materials in the Presence of Nano and Microparticle Additives." Georgia Institute of Technology.

Kevern, J T, and C Farney. 2012. "Reducing Curing Requirements for Pervious Concrete with a Superabsorbent Polymer for Internal Curing." *Transportation Research Record,* 115–21. doi:10.3141/2290-15.

Kevern, J. T., V. R. Schaefer, K. Wang, and M. T. Suleiman. 2008. "Pervious Concrete Mixture Proportions for Improved Freeze-Thaw Durability." *Journal of ASTM International* 5 (2): 101320. doi:10.1520/JAI101320.

Kevern, J. T., K. Wang, and V. R. Schaefer. 2010. "Effect of Coarse Aggregate on the Freeze-Thaw Durability of Pervious Concrete." *Journal of Materials in Civil Engineering* 22 (May): 469–75. doi:10.1061/(ASCE)MT.1943-5533.0000049.

Kevern, John T. 2014. "Climate Change, Energy, Sustainability and Pavements," 261–73. doi:10.1007/978-3-662-44719-2.

Kevern, John T., and Vernon R. Schaefer. 2013. "Mixture Proportioning Considerations for Improved Freeze-Thaw Durability of Pervious Concrete." *ISCORD,* 471–81. http://dx.doi.org/10.1061/9780784412978.046.

Lee, Bo Yeon, and Kimberly E. Kurtis. 2012. "Proposed Acceleratory Effect of TiO 2 Nanoparticles on Belite Hydration: Preliminary Results." *Journal of the American Ceramic Society* 95: 365–68. doi:10.1111/j.1551-2916.2011.04937.x.

Mahboub, K. C., Jonathan Canler, Robert Rathbone, Thomas Robi, and Blake Davis. 2009. "Pervious Concrete: Compaction and Aggregate Gradation." *ACI Materials Journal* 106 (106): 523–28.

Meininger, R. C. 1988. "No-Fines Pervious Concrete for Paving." *Concrete International* 10 (August): 20–27.

Mitchell, M. R., R. E. Link, Jiusu Li, and Zhaohui Liu. 2011. "Microanalysis of Recycled Coarse Aggregate and Properties of No-Fines Pervious Recycled Concrete." *Journal of Testing and Evaluation* 39 (5): 103417. doi:10.1520/JTE103417.

Montes, Felipe, and Liv Haselbach. 2006. "Measuring Hydraulic Conductivity in Pervious Concrete." *Environmental Engineering Science* 23 (6): 960–69. doi:10.1089/ees.2006.23.960.

Mulligan, Ann. 2005. "Attainable Compressive Strength of Pervious Concrete Paving Systems." University of Central Florida. http://etd.fcla.edu/CF/CFE0000634/Mulligan_Ann_M_200508_MS.pdf.

National Ready Mixed Concrete Association (NRMCA). 2014. *Pervious Concrete: Mixture Proportioning Software* (computer software), Silver Spring.

Neithalath, Narayanan. 2004. "Development and Characterization of Acoustically Efficient Cementitious Materials. PhD Thesis." Purdue University. https://engineering.purdue.edu/~concrete/students/Narayanan_Neithenalath_Thesis.pdf.

Nemirovsky, E. M., A. L. Welker, and R. Lee. 2013. "Quantifying Evaporation from Pervious Concrete Systems: Methodology and Hydrologic Perspective." *Journal of Irrigation and Drainage Engineering-ASCE* 139 (4): 271–77.

Park, Seung Bum, Dae Seuk Seo, and Jun Lee. 2005. “Studies on the Sound Absorption Characteristics of Porous Concrete Based on the Content of Recycled Aggregate and Target Void Ratio.” *Cement and Concrete Research* 35: 1846–54. doi:10.1016/j.cemconres.2004.12.009.

Putman, Bradley J., and Andrew I. Neptune. 2011. “Comparison of Test Specimen Preparation Techniques for Pervious Concrete Pavements.” *Construction and Building Materials* 25 (8): 3480–85. doi:10.1016/j.conbuildmat.2011.03.039.

Qing, Ye, Zhang Zenan, Kong Deyu, and Chen Rongshen. 2007. “Influence of Nano-SiO2 Addition on Properties of Hardened Cement Paste as Compared with Silica Fume.” *Construction and Building Materials* 21 (3): 539–45. doi:10.1016/j.conbuildmat.2005.09.001.

Ramirez, Anibal Maury, Kristof Demeestere, Nele De Belie, Tapio Mäntylä, and Erkki Levänen. 2010. “Titanium Dioxide Coated Cementitious Materials for Air Purifying Purposes: Preparation, Characterization and Toluene Removal Potential.” *Building and Environment* 45 (4). Elsevier Ltd: 832–38. doi:10.1016/j.buildenv.2009.09.003.

Rizvi, Rabiah, Susan Tighe, Vimy Henderson, and Jodi Norris. 2010. “Evaluating the Use of Recycled Concrete Aggregate in Pervious Concrete Pavement.” *Transportation Research Record: Journal of the Transportation Research Board* 2164: 132–40. doi:10.3141/2164-17.

Ruot, Bertrand, Arnaud Plassais, François Olive, Laurent Guillot, and Laurent Bonafous. 2009. “TiO2-Containing Cement Pastes and Mortars: Measurements of the Photocatalytic Efficiency Using a Rhodamine B-Based Colourimetric Test.” *Solar Energy* 83: 1794–1801. doi:10.1016/j.solener.2009.05.017.

Senff, L., D. Hotza, S. Lucas, V.M. Ferreira, and J.a. Labrincha. 2012. “Effect of Nano-SiO2 and Nano-TiO2 Addition on the Rheological Behavior and the Hardened Properties of Cement Mortars.” *Materials Science and Engineering: A* 532. Elsevier B.V.: 354–61. doi:10.1016/j.msea.2011.10.102.

Shen, Shihui, Maria Burton, Bertram Jobson, and Liv Haselbach. 2012. “Pervious Concrete with Titanium Dioxide as a Photocatalyst Compound for a Greener Urban Road Environment.” *Construction and Building Materials* 35. Elsevier Ltd: 874–83. doi:10.1016/j.conbuildmat.2012.04.097.

Starke, P., P. Gobel, and W. G. Coldeway. 2010. “Urban Evaporation Rates for Water Permeable Pavements.” *Water Science and Technology* 62 (5): 1161–69.

Suleiman, M. T., J Kevern, V. R. Schaefer, and K Wang. 2006. “Effect of Compaction Energy on Pervious Concrete Properties.” *Concrete Technology Forum-Focus on Pervious Concrete, National Ready Mix Concrete Association*, 1–8. http://www.rmc-foundation.org/images/PCRC Files/Construction Techniques/Effect of Compaction Energy on Pervious Concrete Properties.pdf.

Tarnai, M, H Mizuguchi, S Hatanaka, H Katahira, T Nakazawa, K Yanagibashi, Takenaka Corporation, and M Kunieda. 2003. “Design, Construction and Recent Applications of Porous Concrete in Japan.” In *Our World in Concrete and Structures*. Singapore.

Tho-in, T, and V Sata. 2011. “Pervious High-Calcium Fly Ash Geopolymer Concrete.” *Construction and Building Materials* 30: 366–71. http://www.sciencedirect.com/science/article/pii/S0950061811007057.

Tittarelli, F., M. Carsana, and M. L. Ruello. 2014. “Effect of Hydrophobic Admixture and Recycled Aggregate on Physical-Mechanical Properties and Durability Aspects of No-Fines Concrete.” *Construction and Building Materials* 66. Elsevier Ltd: 30–37. doi:10.1016/j.conbuildmat.2014.05.043.

Vancura, Mary, Kevin MacDonald, and Lev Khazanovich. 2011. “Microscopic Analysis of Paste and Aggregate Distresses in Pervious Concrete in a Wet, Hard Freeze Climate.” *Cement and Concrete Composites* 33 (10). Elsevier Ltd: 1080–85. doi:10.1016/j.cemconcomp.2011.05.011.

Welker, A. L., J. D. Barbis, and P. A. Jeffers. 2012. “A Side-by-Side Comparison of Pervious Concrete and Porous Asphalt.” *Journal of the American Water Resources Association* 48 (4): 809–19.

Xu, Peng, and Boming Yu. 2008. “Developing a New Form of Permeability and Kozeny-Carman Constant for Homogeneous Porous Media by Means of Fractal Geometry.” *Advances in Water Resources* 31: 74–81. doi:10.1016/j.advwatres.2007.06.003.

Yang, Zhifu. 2011. “Freezing-and-Thawing Durability of Pervious Concrete under Simulated Field Conditions.” *ACI Materials Journal* 108 (108): 187–95.

Yousefi, Azam, Ali Allahverdi, and Parisa Hejazi. 2013. “Effective Dispersion of Nano-TiO2 Powder for Enhancement of Photocatalytic Properties in Cement Mixes.” *Construction and Building Materials* 41: 224–30. doi:10.1016/j.conbuildmat.2012.11.057.

Appendix A Mortar Specimen Stress-Strain Curves

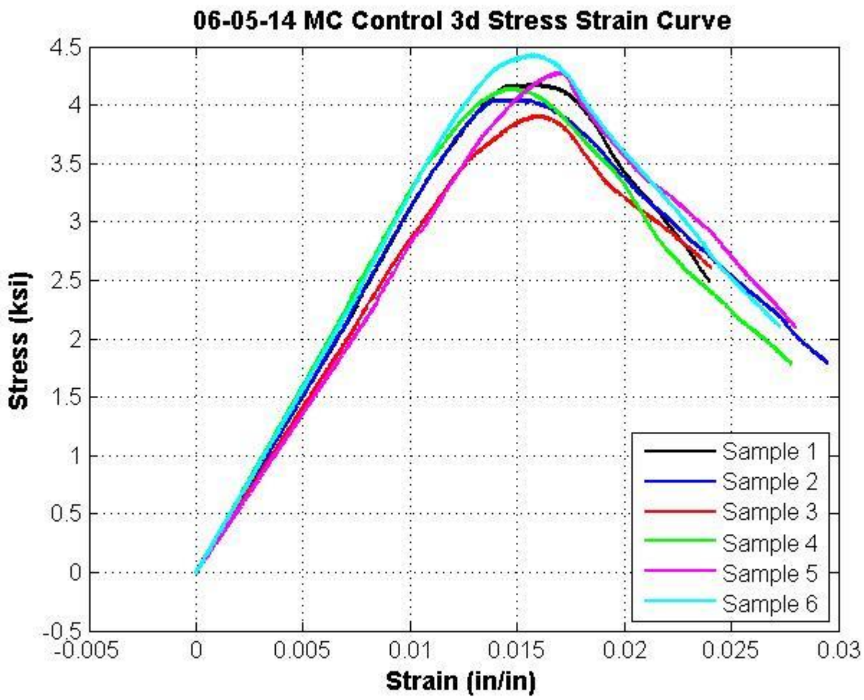

Figure A.1—Stress-Strain Curves for 3-day Control Mortar Samples [1 ksi = 6.9 MPa]

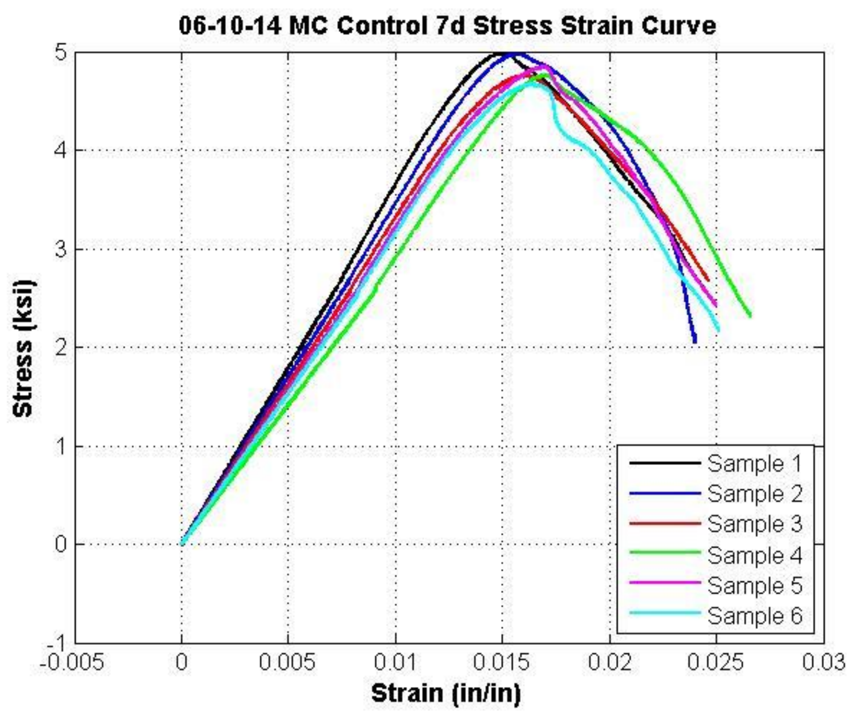

Figure A.2—Stress-Strain Curves for 7-day Control Mortar Samples [1 ksi = 6.9 MPa]

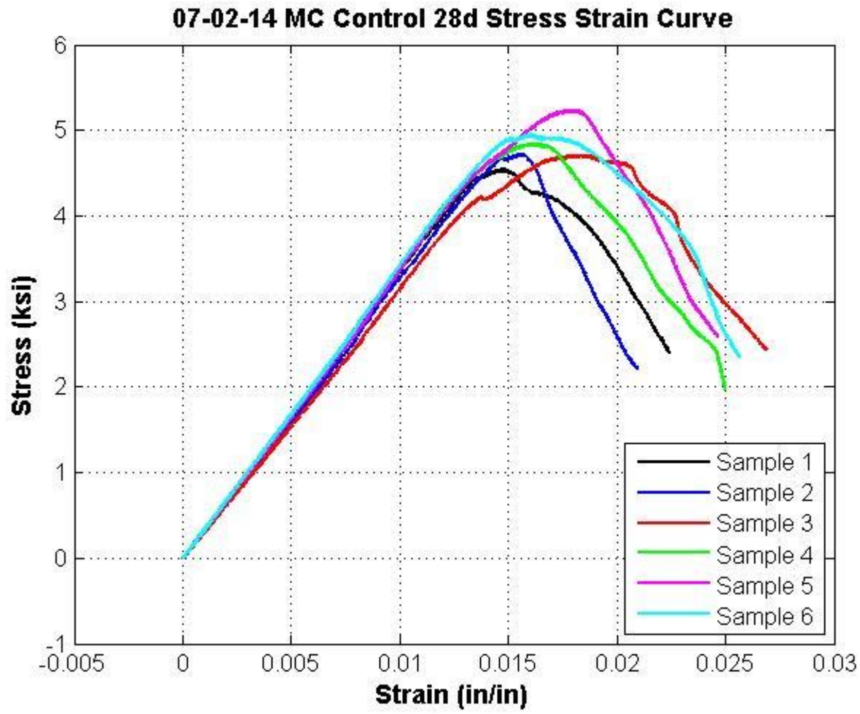

Figure A.3—Stress-Strain Curves for 28-day Control Mortar Samples [1 ksi = 6.9 MPa]

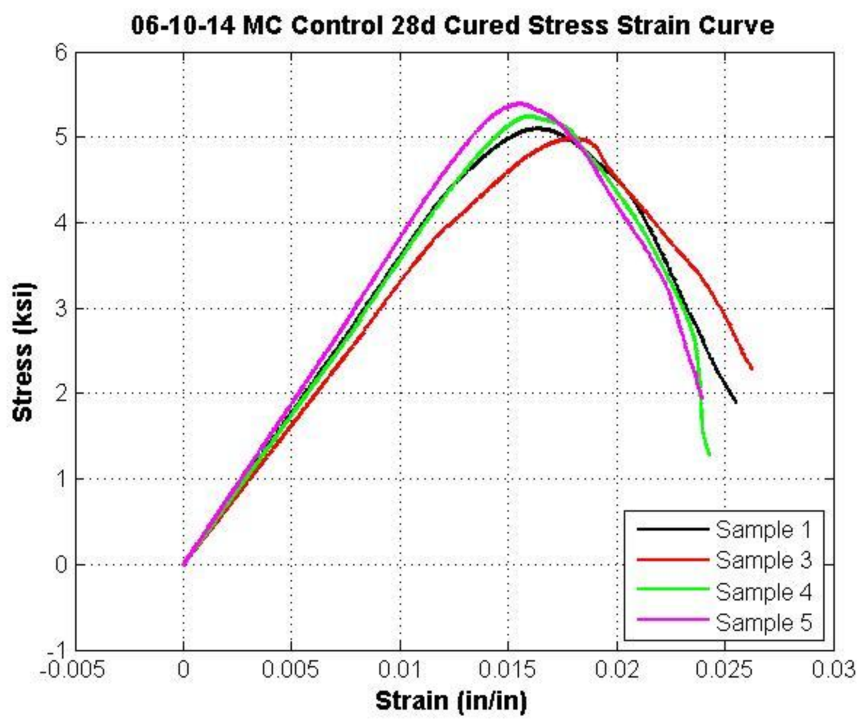

Figure A.4—Stress-Strain Curves for 28-day Cured Control Mortar Samples [1 ksi = 6.9 MPa]

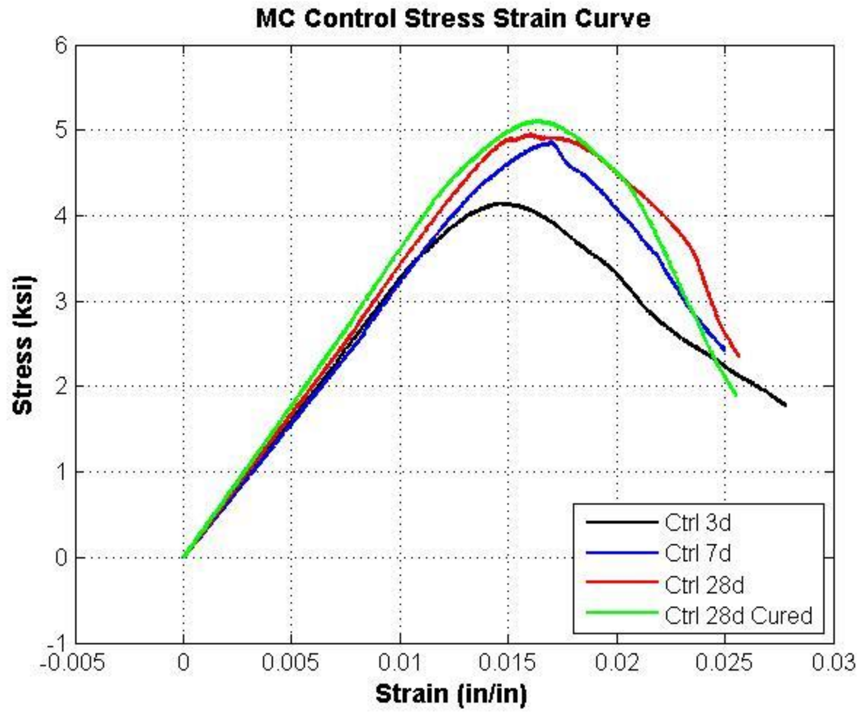

Figure A.5—Comparison of Stress-Strain Curves for Control Mortar Specimens [1 ksi = 6.9 MPa]

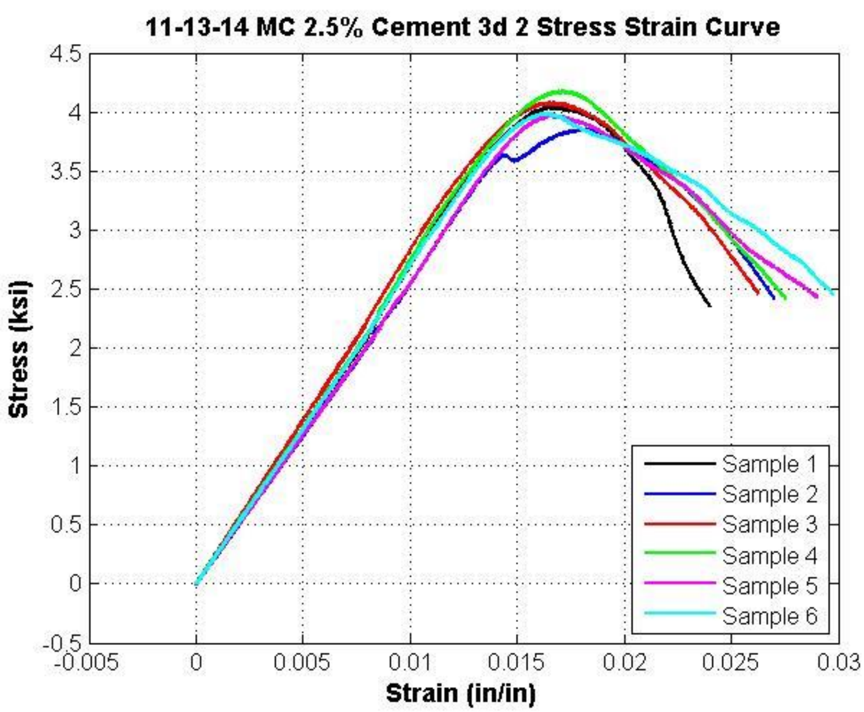

Figure A.6—Stress-Strain Curves for 3-day 2.5C Mortar Samples [1 ksi = 6.9 MPa]

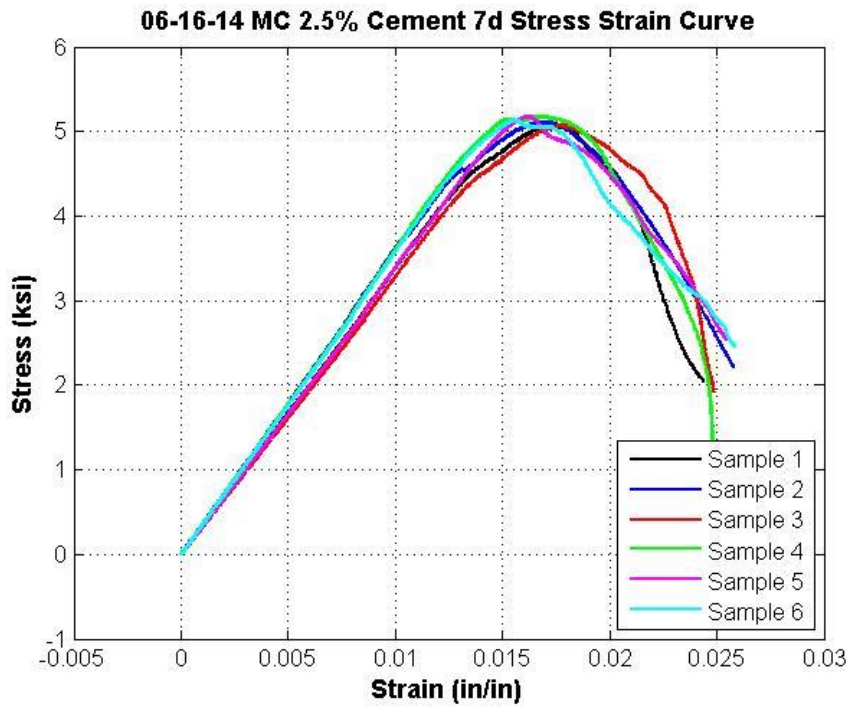

Figure A.7—Stress-Strain Curves for 7-day 2.5C Mortar Samples [1 ksi = 6.9 MPa]

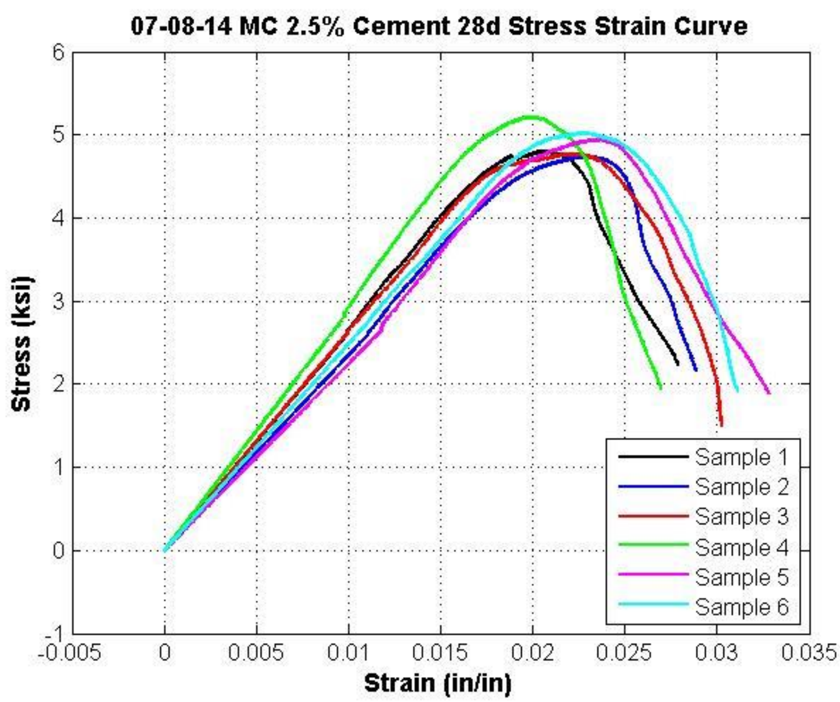

Figure A.8—Stress-Strain Curves for 28-day 2.5C Mortar Samples [1 ksi = 6.9 MPa]

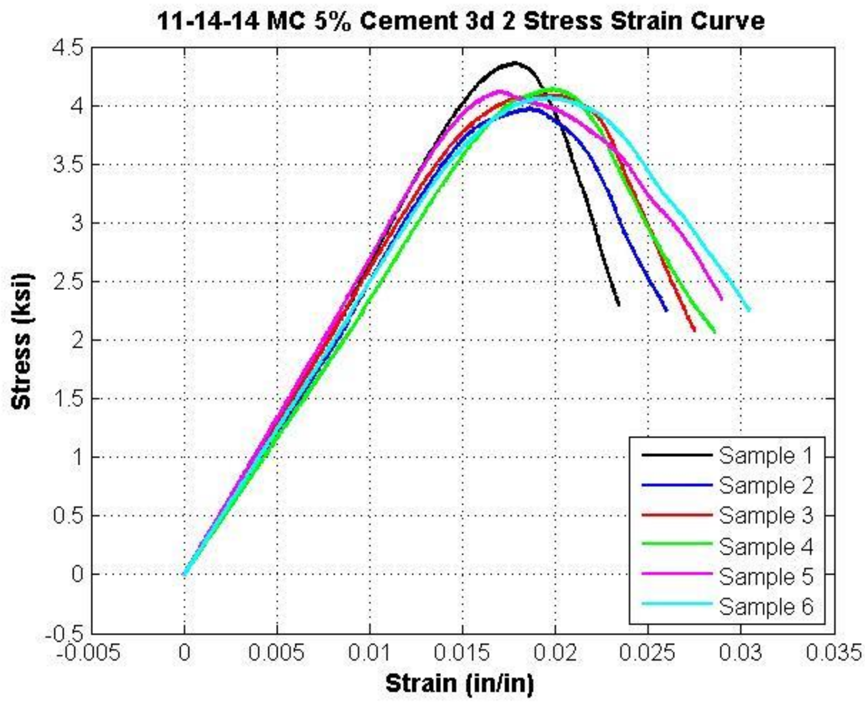

Figure A.9—Stress-Strain Curves for 3-day 5C Mortar Samples [1 ksi = 6.9 MPa]

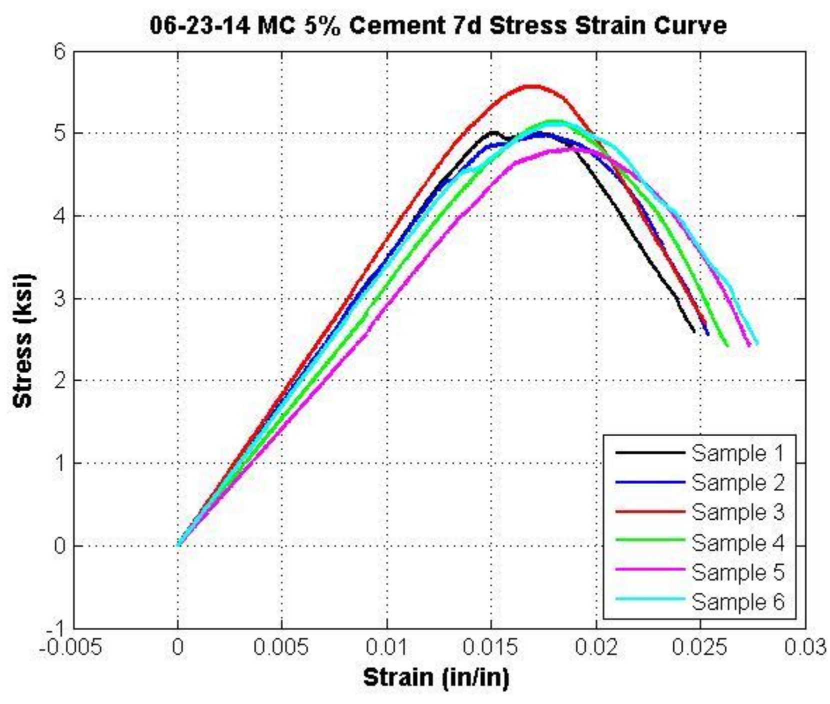

Figure A.10—Stress-Strain Curves for 7-day 5C Mortar Samples [1 ksi = 6.9 MPa]

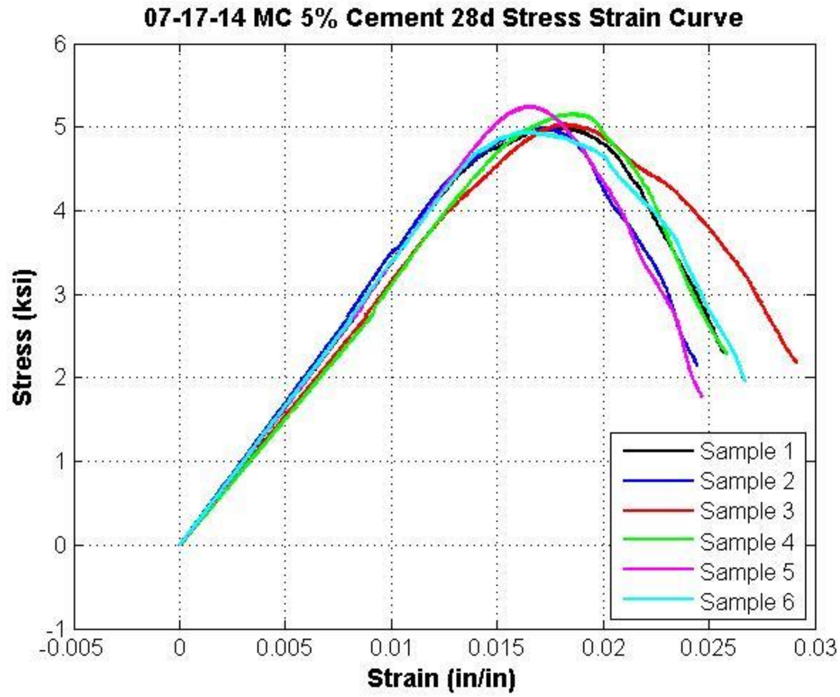

Figure A.11—Stress-Strain Curves for 28-day 5C Mortar Samples [1 ksi = 6.9 MPa]

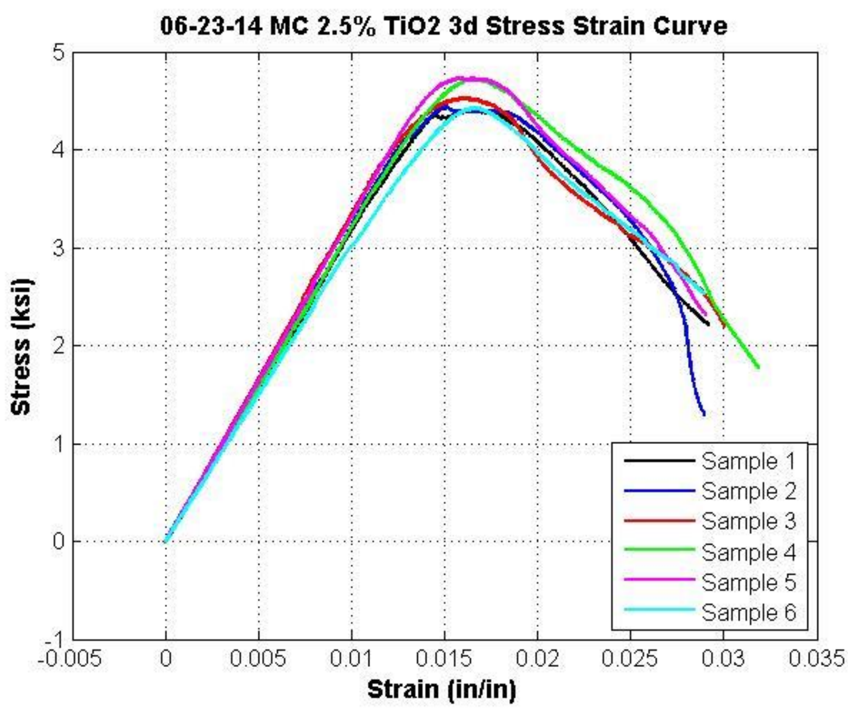

Figure A.12—Stress-Strain Curves for 3-day 2.5T Mortar Samples [1 ksi = 6.9 MPa]

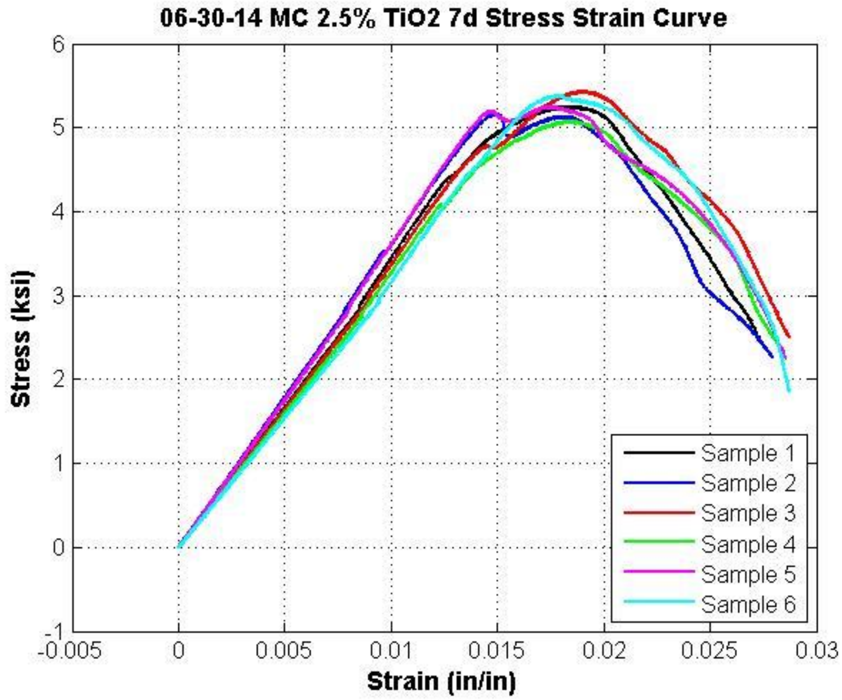

Figure A.13—Stress-Strain Curves for 7-day 2.5T Mortar Samples [1 ksi = 6.9 MPa]

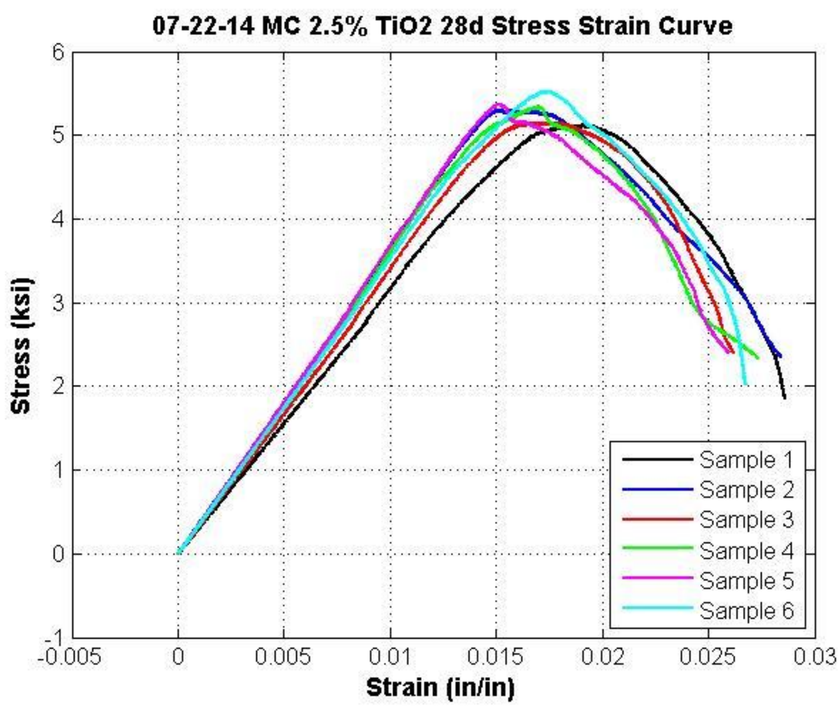

Figure A.14—Stress-Strain Curves for 28-day 2.5T Mortar Samples [1 ksi = 6.9 MPa]

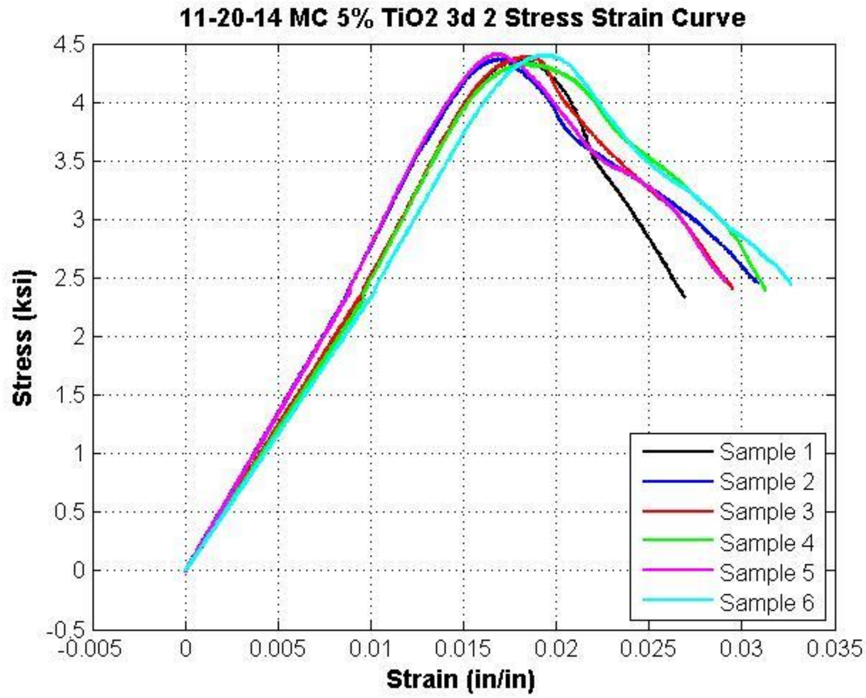

Figure A.15—Stress-Strain Curves for 3-day 5T Mortar Samples [1 ksi = 6.9 MPa]

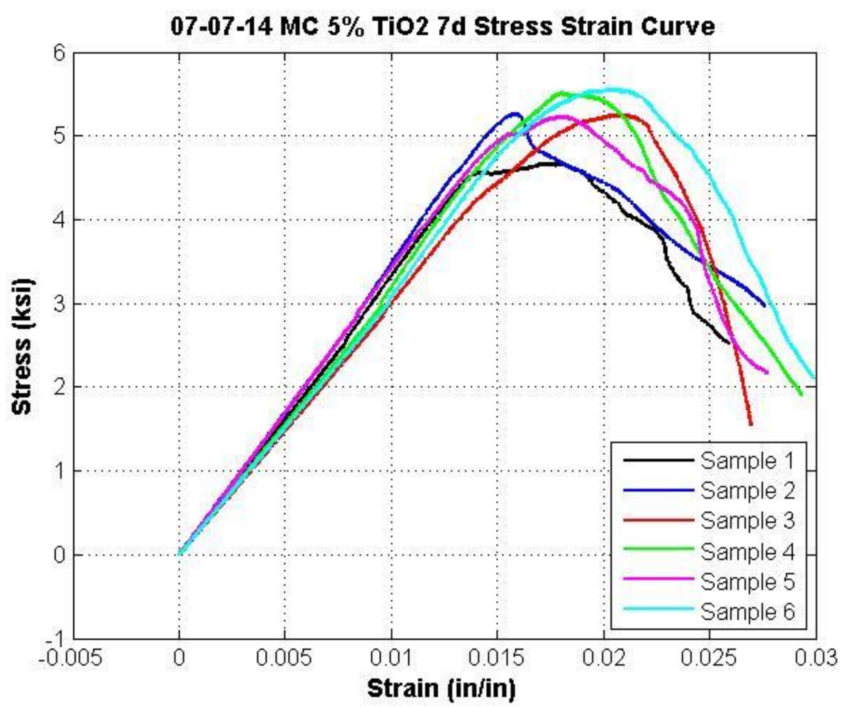

Figure A.16—Stress-Strain Curves for 7-day 5T Mortar Samples [1 ksi = 6.9 MPa]

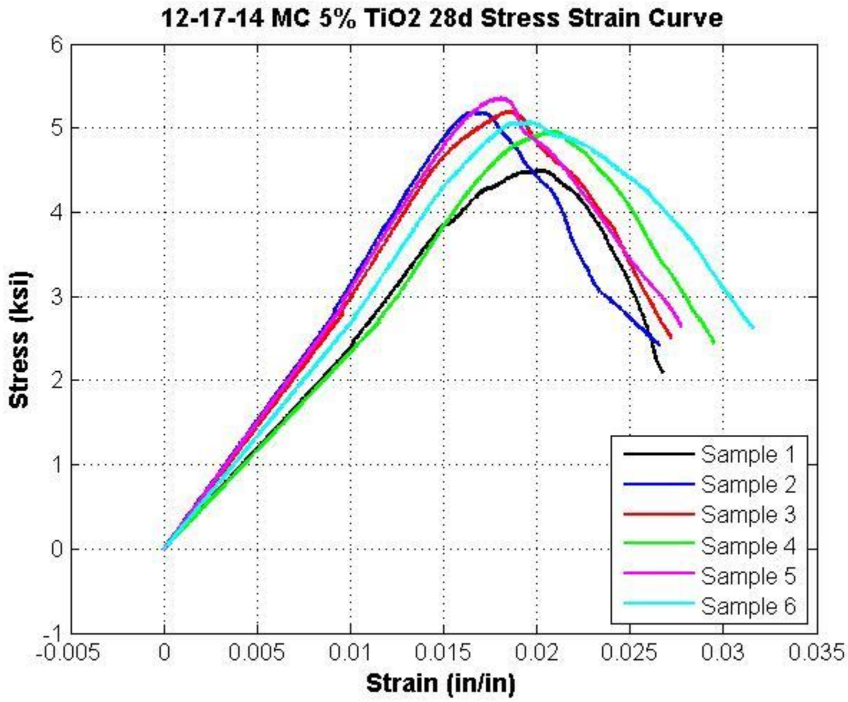

Figure A.17—Stress-Strain Curves for 28-day 5T Mortar Samples [1 ksi = 6.9 MPa]

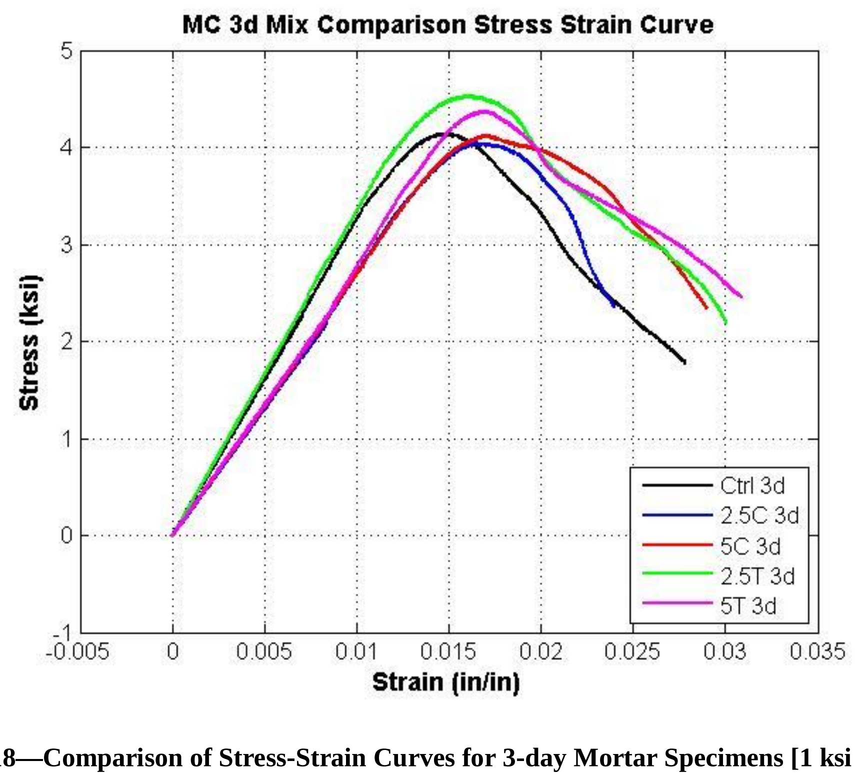

Figure A.18—Comparison of Stress-Strain Curves for 3-day Mortar Specimens [1 ksi = 6.9 MPa]

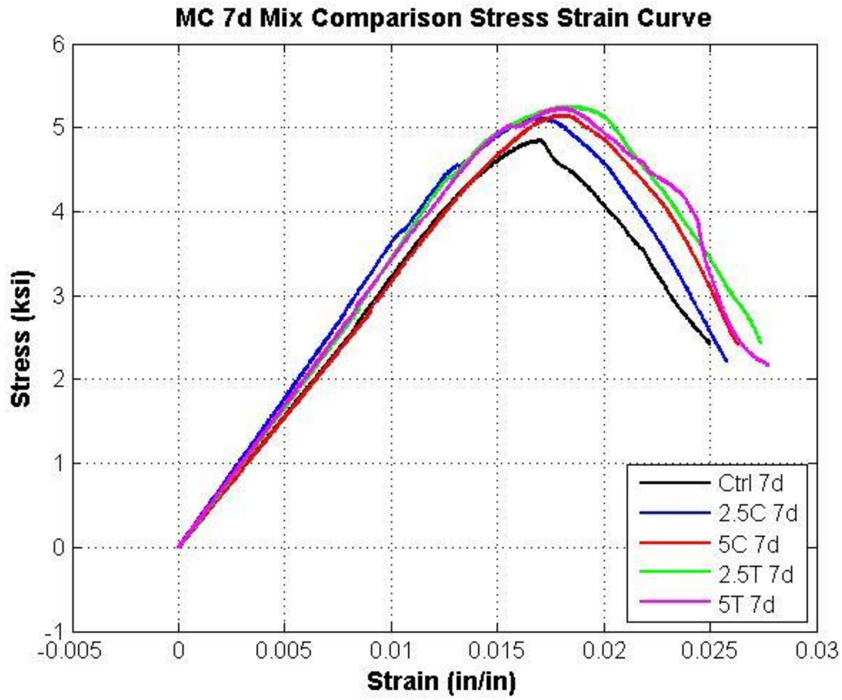

Figure A.19—Comparison of Stress-Strain Curves for 7-day Mortar Specimens [1 ksi = 6.9 MPa]

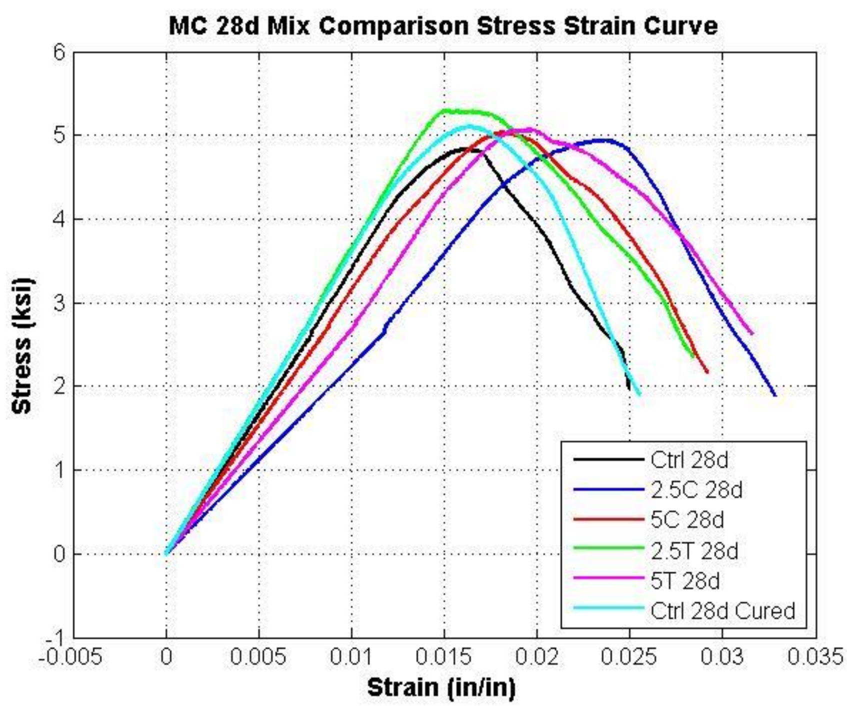

Figure A.20—Comparison of Stress-Strain Curves for 28-day Mortar Specimens [1 ksi = 6.9 MPa]